The Ca^{2+} channel β subunit determines whether stimulation of G$_q$-coupled receptors enhances or inhibits N current

John F. Heneghan,[1,2] Tora Mitra-Ganguli,[1,2] Lee F. Stanish,[1] Liwang Liu,[1,2] Rubing Zhao[1,2], and Ann R. Rittenhouse[1,2]

[1]Department of Physiology and [2]Program in Neuroscience, University of Massachusetts Medical School, Worcester, MA 01655

In superior cervical ganglion (SCG) neurons, stimulation of M$_1$ receptors (M$_1$Rs) produces a distinct pattern of modulation of N-type calcium (N-) channel activity, enhancing currents elicited with negative test potentials and inhibiting currents elicited with positive test potentials. Exogenously applied arachidonic acid (AA) reproduces this profile of modulation, suggesting AA functions as a downstream messenger of M$_1$Rs. In addition, techniques that diminish AA's concentration during M$_1$R stimulation minimize N-current modulation. However, other studies suggest depletion of phosphatidylinositol-4,5-bisphosphate during M$_1$R stimulation suffices to elicit modulation. In this study, we used an expression system to examine the physiological mechanisms regulating modulation. We found the β subunit (Ca$_V$β) acts as a molecular switch regulating whether modulation results in enhancement or inhibition. In human embryonic kidney 293 cells, stimulation of M$_1$Rs or neurokinin-1 receptors (NK-1Rs) inhibited activity of N channels formed by Ca$_V$2.2 and coexpressed with Ca$_V$β1b, Ca$_V$β3, or Ca$_V$β4 but enhanced activity of N channels containing Ca$_V$β2a. Exogenously applied AA produced the same pattern of modulation. Coexpression of Ca$_V$β2a, Ca$_V$β3, and Ca$_V$β4 recapitulated the modulatory response previously seen in SCG neurons, implying heterogeneous association of Ca$_V$β with Ca$_V$2.2. Further experiments with mutated, chimeric Ca$_V$β subunits and free palmitic acid revealed that palmitoylation of Ca$_V$β2a is essential for loss of inhibition. The data presented here fit a model in which Ca$_V$β2a blocks inhibition, thus unmasking enhancement. Our discovery that the presence or absence of palmitoylated Ca$_V$β2a toggles M$_1$R- or NK-1R–mediated modulation of N current between enhancement and inhibition identifies a novel role for palmitoylation. Moreover, these findings predict that at synapses, modulation of N-channel activity by M$_1$Rs or NK-1Rs will fluctuate between enhancement and inhibition based on the presence of palmitoylated Ca$_V$β2a.

INTRODUCTION

All neural function results from a series of electrical and chemical signals. The two realms of signaling are often bridged within neurons by voltage-gated Ca^{2+} channels, such as N channels (West et al., 2001). With depolarization of postsynaptic sites, N-channel activity (N current) triggers biochemical changes, including modulation of certain ion channels (Wisgirda and Dryer, 1994), enzyme activation (Rittenhouse and Zigmond, 1999), and gene transcription (Brosenitsch and Katz, 2001; West et al., 2001; Zhao et al., 2007). In turn, G$_q$ protein-cou-

pled receptors (PCRs) converge on several signal transduction cascades to modulate the N channel's response to changing membrane potential. Some of these pathways are well described, so both signaling molecules and sites of modulation on N channels are known (Suh and Hille, 2005).

A notable exception is the M$_1$ receptor (M$_1$R), a G$_q$PCR that modulates postsynaptic N current by an incompletely described signaling cascade referred to as the slow pathway (Beech et al., 1992; Mathie et al., 1992). Other transmitters such as substance P (SP), the natural ligand for the neurokinin-1 receptor (NK-1R), also modulate N current by a slow pathway (Shapiro and Hille, 1993; Kammermeier et al., 2000) that couples to G$_q$ (Macdonald et al., 1996), suggesting that multiple G$_q$PCRs converge on this pathway (Suh and Hille, 2005). Recent studies propose that a reduction in phosphatidylinositol-4,5-bisphosphate (PtdIns(4,5)P$_2$) levels during G$_q$PCR stimulation suffices for inhibition (Wu et al., 2002; Gamper et al., 2004; Michailidis et al.,

The Rockefeller University Press $30.00
J. Gen. Physiol. Vol. 134 No. 5   369–384
www.jgp.org/cgi/doi/10.1085/jgp.200910203

369

2007). In this model, channels are available to open when PtdIns$(4,5)P_2$ associates with them. During muscarinic stimulation, PtdIns$(4,5)P_2$ is depleted from the membrane, creating a concentration gradient that favors PtdIns$(4,5)P_2$ dissociating and diffusing away from channels. This model appeals to many in part because PtdIns$(4,5)P_2$ dissociation and depletion have been established as the mechanism that inhibits M current, a voltage-gated K^+ current (Suh and Hille, 2002, 2007; Ford et al., 2003; Suh et al., 2006).

However, our previous studies with superior cervical ganglion (SCG) neurons indicate that modulation of native N current by M_1Rs requires events downstream of PtdIns$(4,5)P_2$ hydrolysis (Liu and Rittenhouse, 2003a; Liu et al., 2004, 2008). We found that the muscarinic agonist oxotremorine-M (Oxo-M) and arachidonic acid (AA) elicit the same distinct pattern of modulation (Liu et al., 2001; Liu and Rittenhouse, 2003a), not only inhibiting N current at positive test potentials but also enhancing N current at negative test potentials (Fig. 1 A). Enhancement and inhibition by AA occur at distinct sites and exhibit different biophysical characteristics (Barrett et al., 2001; Liu et al., 2001). Moreover, M_1R stimulation releases AA in central and SCG neurons (Tencé et al., 1994; Liu et al., 2006). In contrast, only minimal fatty acid release occurs after muscarinic stimulation in SCG neurons lacking group IVa PLA$_2$ (Liu et al., 2006). Consistent with the need for PtdIns$(4,5)P_2$ metabolites, inhibiting AA release from phospholipids by antagonizing PLA$_2$ activity or including BSA, a scavenger of AA (Spector, 1975), in the bath solution minimizes N-current modulation by Oxo-M (Liu and Rittenhouse, 2003a; Liu et al., 2003, 2004), suggesting that AA may be a second messenger of the slow pathway.

At present, no binding site for either PtdIns$(4,5)P_2$ or AA on N channels has been determined. Moreover, whether the sites that confer AA sensitivity reside in the same channel or whether two distinct channel populations mediate enhancement and inhibition remains untested. Therefore, we attempted to use the power of mutagenesis to separate enhancement from inhibition in human embryonic kidney 293 (HEK-293) cells expressing recombinant M_1Rs and N channels. N channels are multimeric complexes defined by a large pore-forming subunit (Ca$_V$2.2) that associates with ancillary $\alpha_2\delta$ and Ca$_V\beta$ subunits (Catterall, 2000). We made the serendipitous discovery that enhancement and inhibition separate without mutagenesis simply by expressing different wild-type Ca$_V\beta$s.

MATERIALS AND METHODS

Transfection of HEK-M1 cells
HEK-293 cells with a stably transfected M_1R (HEK-M1; Peralta et al., 1988), a gift from E. Liman (University of Southern California, Los Angeles, CA), were cultured in Dulbecco's modified Eagle's medium/F12 (Invitrogen) supplemented with 10% fetal bovine serum (Invitrogen), 1% G418 (geneticin-selective antibiotic, nonsterile; Invitrogen), and 1% HT supplement (Invitrogen). Cells were transferred into 12-well plates for transfection. Recombinant cells at 50–80% confluence were transfected for 1 h with Ca$_V$2.2 e(Δ24a, +31a, +37b), the N-channel variant found in SCG neurons (Lin et al., 1997); $\alpha_2\delta$-1, which is also expressed in SCG (Lin et al., 2004); and various Ca$_V\beta$s at a 1:1:1 or 1:1:2 molar ratio along with enhanced green fluorescent protein (eGFP) at ~10% of the total DNA using Lipofectamine and PLUS reagent (Invitrogen) as per the manufacturer's instructions. Where noted, the transfection mixture contained expression plasmids encoding 0.028 µg/well NK-1R (UMR cDNA Resource Center, University of Missouri, Rolla, MO). 500–1,000 ng total DNA was transfected per well. 24–48 h after transfection, cells were replated on poly-L-lysine–coated coverslips and allowed to settle for at least 1 h before recording. tsA 201 cells stably transfected with Ca$_V$2.2, $\alpha_2\delta$1, and Ca$_V\beta$3 were provided by D. Lipscombe (Brown University, Providence, RI). These cells were transfected with 500–1,000 ng per well of the M_1R (a gift from N. Nathanson, University of Washington, Seattle, WA) along with eGFP at 10% of the total DNA and processed as described above for current recordings.

Ca$_V\beta$1b (GenBank/EMBL/DDBJ accession no. X61394), Ca$_V\beta$2a (GenBank accession no. M80545), and Ca$_V\beta$4 (GenBank accession no. L02315) were provided by E. Perez-Reyes (University of Virginia, Charlottesville, VA); Ca$_V$2.2 (GenBank accession no. AF055477), $\alpha_2\delta$-1 (GenBank accession no. AF286488), and Ca$_V\beta_3$ (GenBank accession no. M88751) were provided by D. Lipscombe. The Ca$_V\beta$2a(C3,4S) mutant was provided by A. Fox (University of Chicago, Chicago, IL); Ca$_V\beta$2aβ3 and Ca$_V\beta$2aβ1b chimeras were provided by R. Ten Eick (Northwestern University, Evanston, IL). The mutant and chimeric Ca$_V\beta$s were originally made in M. Hosey's laboratory (Northwestern University; Chien et al., 1996, 1998; Chien and Hosey, 1998). Recordings from untransfected HEK-M1 cells yielded whole-cell currents of 9.0 ± 1.3 pA in 20 mM Ba^{2+} (Roberts-Crowley, M., personal communication). To avoid spurious results from endogenous currents, any transfected cells having less than −150 pA were discarded.

Preparation of neonatal rat SCG neurons for electrophysiology
Dissociated sympathetic neurons were obtained from SCG of 1–4-d-old Sprague-Dawley rats (Charles River) according to the methods of Liu and co-workers (Liu et al., 2001; Liu and Rittenhouse, 2003a). To isolate the actions of the slow pathway on N-type current, cells were incubated for at least 5 h with 500 ng/ml pertussis toxin (Biological Laboratories, Inc.) before initiating whole-cell recording experiments (Bernheim et al., 1992). Also, bath solutions included 1 µM of the L-type Ca^{2+} channel antagonist nimodipine to minimize the small amount of L-type current present in SCG neurons. Cells were used within 12 h to avoid recording from cells with processes.

Electrophysiology
Ba^{2+} currents were recorded at room temperature (20–24°C) using the whole-cell configuration of a model 3900a (Dagan), Axon 200A, or Axon 200B (MDS Analytical Technologies) patch-clamp amplifier using methods that were described previously (Barrett et al., 2001; Liu et al., 2001). Currents were filtered at 5 kHz using the amplifier's four-pole low-pass Bessel filter and were digitized at 20 kHz with a micro1401 interface (Cambridge Electronic Design [CED]). Data were collected using Patch 6.4 or Signal 2.15 software suites (CED) and stored on a personal computer. Before analysis, capacitive and leak currents were subtracted using a scaled-up current elicited with a test pulse to −100 mV. Pipette resistance ranged from 2.5 to 5 MΩ. Ba^{2+} currents were elicited every 4 s by stepping from −90 to 0 mV for 100 ms unless

otherwise noted. For cells expressing $Ca_V\beta 2a$, 20 mM Ba^{2+} was used as the charge carrier to improve the signal to noise ratio. The internal solution contained 135 mM Cs-Asp, 10 mM HEPES, 0.1 mM 1,2-bis(O-aminophenoxy)ethane-N,N,N',N'-tetraacetic acid (BAPTA), 5 mM $MgCl_2$, 4 mM ATP, and 0.4 mM GTP, adjusted to pH 7.5 with CsOH. The external solution contained 135 mM N-methyl-D-glutamine-aspartate, 10 mM HEPES, and 5 or 20 mM Ba^{2+} (as indicated), adjusted to pH 7.5 with CsOH. 135 mM N-methyl-D-glutamine-aspartate was substituted for Ba^{2+} when its concentration was lowered from 20 to 5 mM.

Pharmacological agents

Oxo-M (Tocris Biosciences, Inc.) was prepared as a stock solution in double-distilled water and was diluted 1,000 times with bath solution. SP was prepared as a stock solution in 0.05 M acetic acid and diluted at least 2,000 times with bath solution. AA (Nu-Chek Prep), oleyloxyethyl phosphorylcholine (OPC; EMD), and nimodipine were prepared as stock solutions made up in 100% ethanol and diluted 1,000 times with bath solution. All chemicals were obtained from Sigma-Aldrich except where noted.

Data analysis

The Patch 6.4 and Signal 2.15 software were used to measure peak inward current of whole-cell traces. A trough-seeking function was used to determine peak current where indicated. Data were further analyzed using Excel (Microsoft) and Origin 7.0 (OriginLab). Percent inhibition was calculated as $[(I - I')/I] \times 100$, where I is the control current amplitude determined by a mean of five whole-cell current measurements before application of a particular agent and I' is the mean of five current measurements at the time specified for the determination. Conductance was calculated from a modified Ohm's law equation, $G = I/(V_m - V_{rev})$, where I is the peak current at each test potential, V_m is the test potential, and V_{rev} is the apparent reversal potential. Relative conductance curves, (G/G_{max}) − voltage (V_m), were plotted for whole-cell currents before and after AA. Data were curve fit using the Boltzmann equation function in Origin 7.0, yielding a curve fitting the equation $G/G_{max} = G_{max} + (G_{min} - G_{max})/(1 + \exp[(V_m - V_m 1/2)/k])$, where G_{max} is the maximal conductance, G_{min} is the minimal conductance, V_m is the test

distinct site that may be extracellular or in the outer leaflet of the membrane (Barrett et al., 2001). AA inhibits N current by acting at an intracellular site or a site within the inner leaflet (Barrett et al., 2001; Liu et al., 2001). (B) Summary of the percent change in mean current amplitude in tsA 201 cells after 1-min exposure to 10 µM Oxo-M or in HEK-M1 cells in the presence or absence of 10 µM OPC, a PLA_2 antagonist. Error bars represent SEM. (C) Time course of peak inward current using 5 mM Ba^{2+} as charge carrier before, during, and after bath application of 10 µM Oxo-M. (D) Representative whole-cell current traces selected from the respective time course before (black) and 1 min after (red) Oxo-M application. Currents were elicited every 4 s by stepping to a test potential of 0 mV for 100 ms. (E and F) Modulation of N current from tsA 201 cells stably transfected with $Ca_V2.2$, $\alpha_2\delta$-1, and $Ca_V\beta 3$ and transiently transfected with 500–1,000 ng/well of M_1Rs. eGFP is shown in the time course and representative sweeps. The charge carrier was increased to 20 mM Ba^{2+} to improve the signal to noise ratio, and accordingly the test potential was adjusted to 10 mV. (G and H) HEK-M1 cells were transiently transfected with N-channel subunits $Ca_V2.2$, $\alpha_2\delta$-1, and $Ca_V\beta 2a$. Modulation of N current by M_1R stimulation illustrated in a time course (G) and current traces (H). (I and J) N-current modulation from cells expressing HEK-M1 cells transfected as for C. Cells were exposed to OPC for at least 3 min before application of Oxo-M. Bars, 0.4 nA.
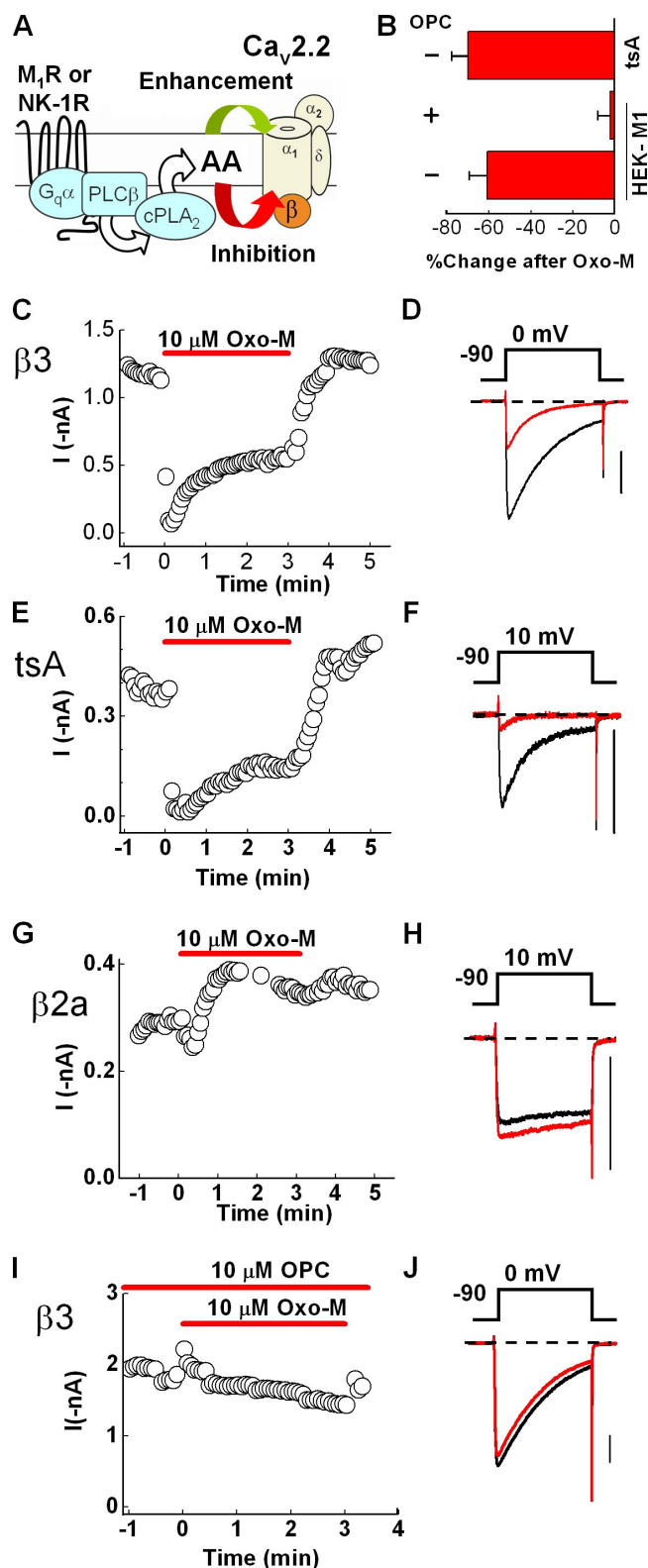
Figure 1. M_1R-induced inhibition of recombinant N current is blocked by a PLA_2 antagonist. HEK-M1 cells were transiently transfected with N-channel subunits $Ca_V2.2$, $\alpha_2\delta$ -1, and $Ca_V\beta 3$. (A) Working model of the slow pathway in which AA release, catalyzed by PLA_2, is a necessary component to elicit N-current modulation. AA enhances current (green arrow) by acting at a

Heneghan et al. 371

potential, $V_m1/2$ is the voltage at half-maximal conductance, and k is the slope factor.

Immunocytochemistry of $Ca_V\beta$ subunits

Adult SCG neurons were plated on chamber slides (Nagle Nune International), treated with poly-L-lysine, and cultured overnight. Cells were washed with PBS twice for 5 min and fixed with 100% acetone for 10 min. The fixative was washed away with PBS at room temperature three times for 5 min. Cells were then exposed to PBS containing 10% normal goat serum for 60 min at room temperature followed by incubation with primary antibody for 60 min at room temperature. Mouse anti-$Ca_V\beta2$ (NeuroMab), rabbit anti-Cav$\beta3$ (Sigma-Aldrich), and mouse anti-Cav$\beta4$ (Neuro-Mab) were diluted 1:1,000 in Antibody Diluent (Dako). Thereafter, cells were washed with PBS three times for 5 min and were incubated for 60 min in the dark at room temperature with Alexa Fluor 488 anti–mouse antibody or Alexa Fluor 488 anti–rabbit antibody (Invitrogen) diluted 1:200 in Antibody Diluent. After incubation with secondary antibodies, cells were washed with PBS three times for 5 min. A second fixation was performed. Slides were then washed with distilled water and covered with the aqueous mounting medium Prolong Gold Antifade reagent (Invitrogen). Images of immunofluorescence were obtained at room temperature using a custom-built, video-rate confocal microscope (Sanderson and Parker, 2003) with a 40× objective lens. An excitation wavelength of 488 nm was used, and emission spectra were collected with long-pass filters (OGSIS) at 515 nm (Perez and Sanderson, 2005).

RT-PCR of $Ca_V\beta$ subunits

Homogenized tissue samples were lysed in 0.8 ml TRIZOL reagent (Invitrogen), and DNA was removed from RNA using phenol-chloroform phase separation. Next, RNA was precipitated using isopropyl alcohol and washed with 75% ethanol. After drying, the RNA pellet was dissolved in RNase-free water. Subsequently, reverse transcription was performed using 1.0 µl of 10× buffer reverse transcriptase, 1.0 µl deoxyribonucleotide triphosphate (dNTP) mix (5 mM each of dNTP), 1.0 µl oligo-dT primer (0.5 mg/ml), 0.125 µl RNase inhibitor (40 U/µl; Promega), 0.5 µl Omniscript Reverse transcription, and RNase-free water to make up a total volume of 10 µl (all reagents were obtained from QIAGEN unless otherwise noted). The mixture was incubated at 37°C for 1 h and heated at 93°C for 5 min followed by cooling on ice to rapidly inactivate the transcriptase. Aliquots of reverse transcription PCR product were amplified by PCR using the primers $Ca_V\beta2a$ (5′-ATAACCACAGAGAGGAGAGCCACA-3′ and 5′-TATACATCCCTGTTCCACTCGCCA-3′; 258-bp product) and $Ca_V\beta3$ (5′-TCCCTGGACTTCAGAACCAGCAG-3′ and 5′-TTGT-GGTCATGCTCCGAGTCCTG-3′; 368 bp; Lin et al., 1996). Reaction mixtures for PCR contained 2 µl of template cDNA, 2.5 µl of 10× buffer, 0.5 µl dNTP mix, and 2 µl each of forward and reverse primer and were made up in distilled water to a final volume of 25 µl. The protocol for amplification was 94°C for 4 min followed by 33 cycles of 94°C for 45 s, 60°C for 45 s, 72°C for 1 min, and holding at 72°C for 10 min for last extension. PCR products were run on 1.8% agarose gel stained with ethidium bromide along with a 1,000-bp DNA ladder (Fermentas Life Sciences).

Statistical analysis

Summary data are presented as means ± SEM. A two-tailed paired *t* test was used to determine differences between control and agonist. For comparisons of two different groups, data were analyzed by a two-tailed Student's *t* test for two means. For multiple comparisons, statistical significance was determined using Origin 7.0 by a one-way ANOVA followed by a Tukey multiple comparison posthoc test. Statistical significance was set at $P \leq 0.05$.

Online supplemental material

Fig. S1 shows that exogenous application of AA inhibits N-type current in SCG neurons. The L-type channel agonist FPL 64176 was used to distinguish effects of AA on N current from L current. The AA analogue ETYA (5,8,11,14-eicosatetraynoic acid) was used to block metabolism of AA. Fig. S2 demonstrates that the enhancing and inhibiting effects of AA are reversible using an application of fatty acid–free BSA subsequent to AA application. Fig. S3 shows that in HEK-M1 cells transfected with $Ca_V2.2$, $\alpha_2\delta$-1, $Ca_V\beta2a$, and $Ca_V\beta3$, both enhancement and inhibition of N current occurs during application of AA. Online supplemental material is available at http://www.jgp.org/cgi/content/full/jgp.200910203/DC1.

RESULTS

To test whether a homogeneous population of N channels recapitulates both enhancement and inhibition, N currents were screened for modulation by Oxo-M. Recombinant currents were evoked from HEK-M1 cells transiently transfected with N-channel subunits $Ca_V2.2$, $\alpha_2\delta$-1, and $Ca_V\beta3$, which most commonly associates with $Ca_V2.2$ (Witcher et al., 1993). Oxo-M rapidly inhibited peak inward current, reaching a stable inhibition within 90 s (Fig. 1, B–D). Because N-current enhancement is voltage dependent (Liu and Rittenhouse, 2003a), we compared current–voltage (I-V) plots measured before and after Oxo-M, expecting to observe current enhancement at negative test potentials. However, Oxo-M inhibited current at virtually all voltages (Fig. 2 C). tsA 201 cells stably transfected with the same subunits exhibited a similar profile of inhibition after exposure to Oxo-M (Fig. 1, B, E, and F), ruling out a system-specific effect.

$Ca_V\beta$ subunit controls N-current modulation by G_qPCRs

Lack of enhancement at any potential indicated the recombinant system was fundamentally different from N-current modulation observed in SCG neurons. In addition to incomplete recapitulation of G_qPCR modulation, recombinant N current exhibited robust, fast inactivation (Fig. 1, D and F, and Fig. 2 C) as previously observed with channels containing $Ca_V\beta3$ (Olcese et al., 1994). In contrast, native N current in SCG neurons exhibits kinetics with little inactivation (Plummer et al., 1989), similar to recombinant N current from channels containing $Ca_V\beta2a$ (Hurley et al., 2000; Yasuda et al., 2004). Moreover, AA robustly inhibits noninactivating current in SCG neurons evoked with a test pulse duration ranging from 20 (Fig. S1) to 700 ms (Liu and Rittenhouse, 2000; Liu et al., 2001). Because SCG neurons express $Ca_V\beta2$ mRNA (Lin et al., 1996), we hypothesized that the majority of N current arises from $Ca_V\beta2a$-containing channels. If true, these channels might exhibit both inhibition and enhancement. We found that Oxo-M rapidly inhibited N current from cells expressing $Ca_V\beta2a$. However, unlike $Ca_V\beta3$, initial inhibition gave way to stable enhancement (Fig. 1, G and H). Moreover, comparison of I-V plots revealed
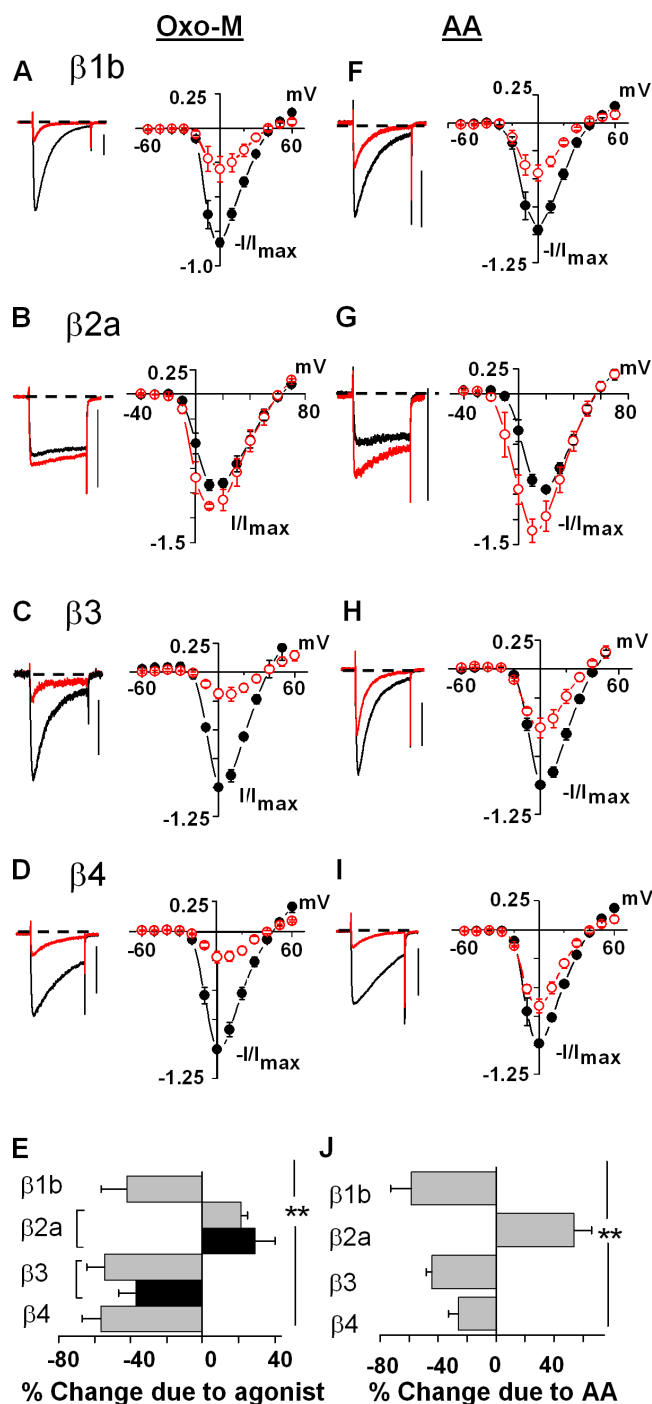
that Oxo-M no longer inhibited current at any potential but enhanced current at negative test potentials (Fig. 2 B). Although we hypothesized that expression of $Ca_V\beta2a$ would elicit enhancement at negative potentials, separation of enhancement from inhibition based on $Ca_V\beta$ expression was unanticipated. Therefore, we tested whether other $Ca_V\beta$s would dually modulate N current by repeating the aforementioned experiments with two other neuronal $Ca_V\beta$s: $Ca_V\beta1b$ and $Ca_V\beta4$. As with $Ca_V\beta3$, when either $Ca_V\beta1b$ (Fig. 2 A) or $Ca_V\beta4$ (Fig. 2 D) was expressed, Oxo-M inhibited current at all test potentials, indicating that channels containing $Ca_V\beta2a$ exhibit unique N-current modulation by M_1Rs.

To determine whether M_1Rs uniquely influence the profile of modulation, we examined whether N-current modulation by another G_qPCR depends on $Ca_V\beta$. We tested NK-1Rs because in SCG neurons, stimulation of M_1Rs and NK-1Rs inhibits N current through converging signaling pathways that require $G\alpha_q$ and downstream activation of PLC (Shapiro et al., 1994; Kammermeier et al., 2000; Liu and Rittenhouse, 2003a). We examined current modulation that occurred after exposure to SP. As with Oxo-M, an initial transient inhibition progressed to a stable current enhancement when $Ca_V\beta2a$ was expressed along with $Ca_V2.2$ and $\alpha_2\delta$-1 (Fig. 3, A and C). In contrast, SP elicited sustained inhibition with $Ca_V\beta3$ expression (Fig. 2 E and Fig. 3, B and C). These data indicate that control of modulation by $Ca_V\beta$ is a mechanism used by other G_qPCRs rather than being unique to M_1Rs (Fig. 1 A).

AA elicits a profile of N-current modulation similar to G_qPCR stimulation

AA mimics N-current modulation by M_1Rs in SCG neurons and may serve as a downstream messenger of this pathway (Liu and Rittenhouse, 2003a). If so, AA also should inhibit or enhance recombinant N current similarly to M_1R or NK-1R stimulation. When this hypothesis was tested, AA's actions recapitulated the pattern of modulation observed with M_1R or NK-1R stimulation: enhancement and inhibition separated based on $Ca_V\beta$ expression (Fig. 2, F–J). If elevated AA levels mediate enhancement and inhibition, both should reverse after washout of exogenous AA. As with SCG neurons, washing with copious amounts of bath solution or with 1 mg/ml BSA reversed modulation (Fig. S2, A–F). Moreover, enhancement recurred with a second application of AA after washing with BSA (Fig. S2 A). These findings

Figure 2. $Ca_V\beta$ determines N-current modulation by G_qPCRs and AA. (A–D) HEK-M1 cells were transiently transfected with $Ca_V2.2$, $\alpha_2\delta$-1, and various $Ca_V\beta$ subunits. Currents, measured in 5 mM $[Ba^{2+}]$, were elicited every 4 s by stepping from −90 to 0 mV for 100 ms unless otherwise noted. Representative whole-cell current traces were always taken before (black) and 3 min after (red) drug application. Averaged normalized I-V plots were taken before (black closed circles) and 90 s after (red open circles) agonist application. n = 3–6 cells per group. For cells expressing $Ca_V\beta2a$, 20 mM $[Ba^{2+}]$ was used as charge carrier to improve the signal to noise ratio. The test potential was adjusted to 10 mV to correct for the shift in peak inward current. (E) Histogram summarizing N-current modulation after 3 min of 10 µM Oxo-M (gray bars) and 5 nM SP (black bars). Percent change in current amplitude was highly significant between $Ca_V\beta2a$ and $Ca_V\beta1b$, $Ca_V\beta3$, or $Ca_V\beta4$ irrespective of whether Oxo-M or SP was applied (**, P < 0.005; one-way ANOVA). (F–I) Modulation of N current by 10 µM AA shown as current traces and averaged I-V plots (n = 4–5 cells per group). (J) Histogram summarizing N-current modulation after 3 min of AA (**, P < 0.005; one-way ANOVA). Error bars represent SEM. Bars, 0.4 nA.
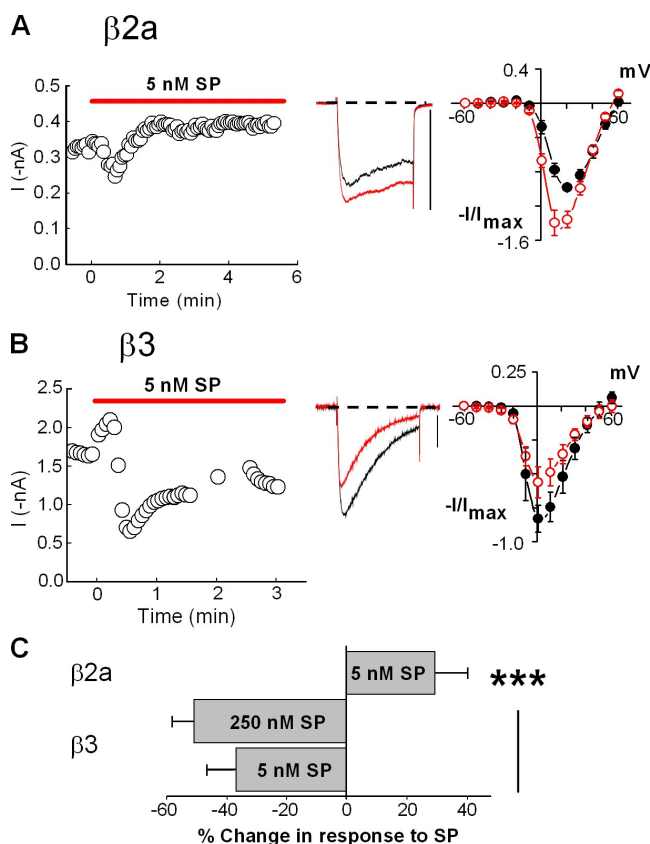
A β2a

B β3

C

Figure 3. NK-1R stimulation elicits a similar profile of N-current modulation as M_1Rs. (A and B) HEK-M1 cells were transiently transfected with the NK-1R along with $Ca_V2.2$, $\alpha_2\delta$-1, and either $Ca_V\beta2a$ (A) or $Ca_V\beta3$ (B). Using 5 nM SP as the agonist, current modulation is shown in a time course of peak current (left), representative whole-cell current traces (middle), and averaged I-V plots (right; $n = 4$). Bars, 0.4 nA. (C) Summary of the modulatory effects of SP on currents from cells expressing either $Ca_V\beta2a$ or $Ca_V\beta3$ (***, $P < 0.005$; one-way ANOVA). No significant difference in current inhibition was observed from cells expressing $Ca_V\beta3$ with 5 and 250 nM SP ($P > 0.26$). Error bars represent SEM.

corroborate our assertion that AA mediates N-current modulation by the slow pathway (Liu and Rittenhouse, 2003a,b; Liu et al., 2004).

As a final test of AA's role in the slow pathway, we antagonized endogenous AA's release from membrane phospholipids using the PLA_2 antagonist OPC. Exposure to Oxo-M for 60 s significantly inhibited N current from $Ca_V\beta3$-containing channels ($P < 0.05$; $n = 16$). In contrast, OPC eliminated significant current inhibition by Oxo-M ($P > 0.05$; $n = 7$; Fig. 1, B, I, and J). A similar profile was observed with SP (not depicted). The striking recapitulation by AA of G_qPCR-induced N-current enhancement and inhibition, coupled with the loss of modulation when antagonizing AA release or sequestering free AA with BSA, advance our previous hypothesis that PLA_2 and AA participate in the slow pathway (Liu and Rittenhouse, 2003a,b; Liu et al., 2004).

Expression of multiple $Ca_V\beta$ isoforms produces heterogeneous N currents

Our findings yield a possible explanation for why SCG neurons exhibit both enhancement and inhibition of whole-cell N current (Barrett et al., 2001; Liu and Rittenhouse, 2003a; Liu et al., 2004). N current's diverse biophysical properties in different neurons have been attributed to $Ca_V2.2$ coexpression with different $Ca_V\beta$ isoforms within individual neurons (Scott et al., 1996). Similarly, SCG neurons may exhibit both forms of modulation because $Ca_V2.2$ coassembles with different $Ca_V\beta$s. If this hypothesis is correct, the pattern of modulation observed in SCG neurons should recapitulate in HEK-M1 cells transfected with multiple $Ca_V\beta$s. When cells were transfected with $Ca_V\beta2a$ and $Ca_V\beta3$, the I-V plots recapitulated I-V plots from SCG neurons (Liu and Rittenhouse, 2003a), with enhancement occurring at negative potentials and inhibition at positive potentials after exogenously applied AA (Fig. S3). However, unlike activity from SCG neurons (Liu et al., 2001; Liu and Rittenhouse, 2003a), the currents rapidly inactivated. It has been reported that SCG neurons from 4-d-old rat pups express $Ca_V\beta2a$, $Ca_V\beta3$, and $Ca_V\beta4$ mRNA with trace amounts of $Ca_V\beta1b$ mRNA (Lin et al., 1996). We verified the presence of $Ca_V\beta2$, $Ca_V\beta3$, and $Ca_V\beta4$ protein in freshly dissociated SCG neurons by immunocytochemistry (Fig. 4 A). Therefore, we retested for the modulatory response in HEK-M1 cells transfected with varying ratios of $Ca_V\beta2a$-, $Ca_V\beta3$-, and $Ca_V\beta4$-transformed plasmid. Transfection with a mixture of cDNAs in the molar ratio of 10:1:1 for $Ca_V\beta2a/Ca_V\beta3/Ca_V\beta4$ in a HEK-M1 cell closely recapitulated the N-current kinetics we had previously observed in SCG neurons (Barrett and Rittenhouse, 2000; Liu and Rittenhouse, 2003a). Application of 10 µM Oxo-M resulted in significant inhibition of currents elicited at test potentials 10–50 mV, with no significant inhibition at lower potentials (Fig. 4 B). To ensure the transfection mixture is an accurate recapitulation of the SCG neuron, we harvested fresh SCG neurons from neonatal rat pups and tested them using the same experimental conditions as we used for the HEK-M1 cells. We found that application of 10 µM Oxo-M also resulted in significant inhibition of native currents elicited at test potentials 10–50 mV, with no significant change at lower potentials (Fig. 4 C). These findings suggest that the N current observed in SCG neurons results from heterogeneous expression of different $Ca_V\beta$ isoforms with $Ca_V2.2$.

The antibody used in the immunocytochemistry experiments recognizes the peptide sequence RSPKP-SANSVTSPHSKE (NeuroMab data sheet N8b_1). This sequence exists in $Ca_V\beta2a$, 2b, 2c, 2d, and 2e but not 2f, 2g, or 2h. Because the presence of $Ca_V\beta2a$ variant has never been confirmed in rat neonatal SCG neurons, we looked for its presence by RT-PCR using primers designed
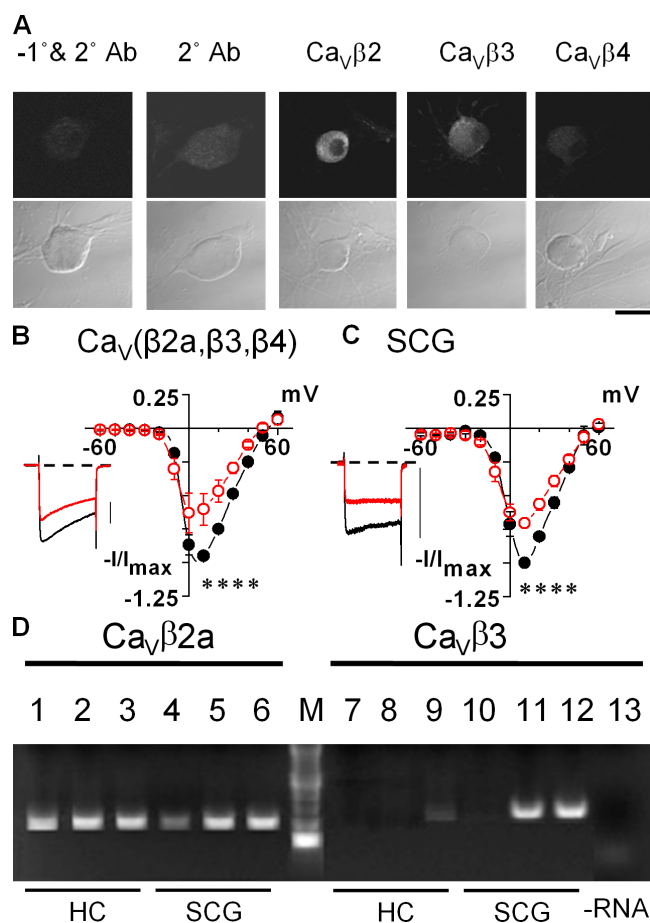
Figure 4. Expression of multiple $Ca_V\beta$ subunits in SCG neurons. (A, top) Confocal micrographs of individual SCG neurons. Starting from the left, the neurons were exposed to no antibodies, secondary antibody (anti–mouse Alexa Fluor 488) only, mouse anti-$Ca_V\beta2$ followed by secondary rabbit anti–mouse Alexa Fluor 488, anti-$Ca_V\beta3$ followed by anti–rabbit Alexa Fluor 488, and mouse anti-$Ca_V\beta2$ followed by secondary antibody. (bottom) Corresponding view shown in bright field. Bar, 10 µm. (B) Representative current traces and mean I-V plots taken from HEK-M1 cells transiently transfected with a 12:12:10:1:1 ratio of $Ca_V2.2/\alpha_2\delta-1/Ca_V\beta2a/Ca_V\beta3/Ca_V\beta4$; taken before (black) and after (red) 10-µM Oxo-M application ($n = 6$ cells). All currents for the figure were recorded using 20 mM Ba^{2+}. *, P < 0.05; paired t test at each test potential. (C) Current traces and mean I-V plots taken from freshly dissociated SCG neurons before (black) and after (red) application of 10 µM Oxo-M ($n = 4$ neurons). Error bars represent SEM. Bars, 0.4 nA. (D) RT-PCR of SCG and hippocampal (HC) homogenates from three different 7-d-old rats comparing $Ca_V\beta2a$ and $Ca_V\beta3$ expression. RNA from animal #1 generated lanes 1, 4, 7, and 10. RNA from animal #2 generated lanes 2, 5, 8, and 11. RNA from animal #3 generated lanes 3, 6, 9, and 12. Lane 13 represents a negative control: RT-PCR reaction without isolated RNA.

specifically for $Ca_V\beta2a$. Using tissue from three different animals, we assessed the presence of $Ca_V\beta2a$ and $Ca_V\beta3$ in SCG. As a positive control, we used the same three animals to run parallel experiments of $Ca_V\beta$ isoform expression in the hippocampus, a region reported to be enriched in $Ca_V\beta2$ (Day et al., 1998). We found $Ca_V\beta2a$ expression

in three of three hippocampal samples and in three of three SCG samples. We also found $Ca_V\beta3$ expression in two of three SCG samples but found negligible $Ca_V\beta3$ expression in hippocampal samples.

A model for dual modulation of N current

We established a working model for how $Ca_V\beta2a$ controls modulation based on previous studies that examined AA's mechanism of inhibition of different Ca^{2+} channels (Barrett et al., 2001; Liu et al., 2001). Our experiments with SCG neurons demonstrated that current inhibition by AA occurs intracellularly or within the inner leaflet of the membrane. In contrast, enhancement appears located extracellularly or within the outer leaflet of the bilayer (Barrett et al., 2001; Liu et al., 2001). $Ca_V\beta$ subunits bind to cytoplasmic loops of $Ca_V2.2$ (Pragnell et al., 1994). Thus, we hypothesized that the unique interactions of $Ca_V\beta2a$ with $Ca_V2.2$ somehow attenuate inhibition. In SCG neurons (Barrett et al., 2001; Liu et al., 2001) and with recombinant channels containing either $Ca_V\beta2a$ or $Ca_V\beta3$ (Fig. 5, A and B), AA induces initial N-current enhancement, which is sustained with $Ca_V\beta2a$ but for $Ca_V\beta3$ is followed by a more slowly progressing inhibition. This observation supports the model. Thus, we postulated that every $Ca_V2.2$ exhibits current enhancement that becomes masked by subsequent, more dominant inhibition.

Because our previous work indicated that enhancement by AA arises from increased voltage sensitivity (Barrett et al., 2001), we compared normalized conductance–voltage (G-V) curves to determine whether increased voltage sensitivity occurs independently of $Ca_V\beta2a$ expression. Both $Ca_V\beta2a$- and $Ca_V\beta3$-containing cells exhibited a negative shift in conductance in response to AA (Fig. 5, C and D), demonstrating that AA increases N-channel voltage sensitivity independently of $Ca_V\beta$ subunit expression. These data suggest that $Ca_V\beta2a$'s unique ability to attenuate inhibition reveals sustained enhancement. In contrast, inhibition results from increased stability of a closed state (Liu and Rittenhouse, 2000), essentially reducing the number of channels available to open. This type of inhibition should dominate an increase in voltage sensitivity; if channels will not open at any voltage, increasing their voltage sensitivity will have little effect on currents. Thus, by blocking a dominating inhibition, $Ca_V\beta2a$ unmasks latent enhancement.

Loss of $Ca_V\beta2a$ palmitoylation restores partial inhibition of N current by Oxo-M or AA

Having established that $Ca_V\beta2a$ uniquely blocks N-current inhibition by G_qPCR stimulation or exogenous AA, we investigated the structural aspects of $Ca_V\beta2a$ to determine its mechanism of action. A conspicuous feature of $Ca_V\beta2a$ is its unique palmitoylation of two cysteine residues near the N terminus (Chien et al., 1996). Our

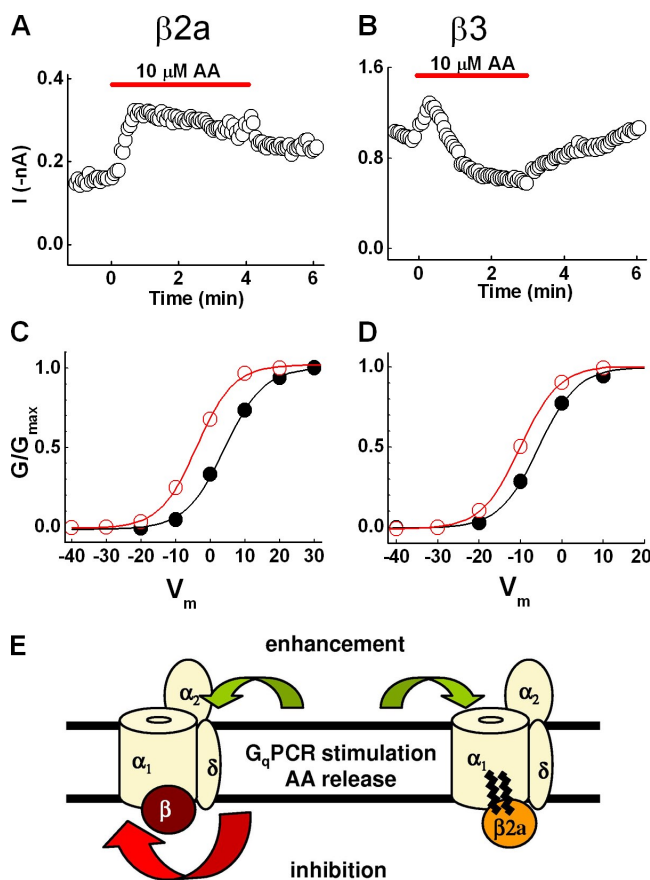**Figure 5.** Ca$_V$β2a blocks N-current inhibition, revealing latent enhancement. (A and B) Time courses of cells expressing either Ca$_V$β2a (A) or Ca$_V$β3 (B) exposed to AA both exhibit enhancement during the initial phase of time course. However, when Ca$_V$β3 is present, inhibition eventually dominates, indicating that both inhibitory and enhancement sites are available for AA to bind. When Ca$_V$β2a is present, inhibition no longer occurs, suggesting the palmitoylated Ca$_V$β2a occupies the inhibitory site without conferring inhibition. (C and D) Normalized conductance–voltage plots generated from I-V data show a negative shift in G/G$_{max}$ for cells expressing either Ca$_V$β2a (C) or Ca$_V$β3 (D), indicating that an increased sensitivity to voltage is masked by a dominating inhibition in cells expressing Ca$_V$β3. (E) Schematic representation of working model. Upon G$_q$PCR stimulation, the released AA binds to both inhibitory and enhancement sites on the channel. When Ca$_V$β3 is present, both inhibitory and enhancement sites are available for AA to bind. However, because inhibition dominates, the resultant modulation observed is current inhibition. When Ca$_V$β2a is present, inhibition no longer occurs because the palmitoylated Ca$_V$β2a occupies the inhibitory site without conferring inhibition. With inhibition antagonized, sustained current enhancement is observed.

observation that palmitoylated Ca$_V$β2a interferes with a fatty acid–mediated inhibition of Ca$_V$2.2 raises the possibility of direct antagonism between palmitic acid and AA (Fig. 5 E). Therefore, we tested a depalmitoylated mutant to determine whether Ca$_V$β2a must be palmitoylated to minimize inhibition and reveal enhancement. Currents from channels containing depalmitoylated Ca$_V$β2a (Ca$_V$β2a[C3,4S]; Chien et al., 1996) exhibited an
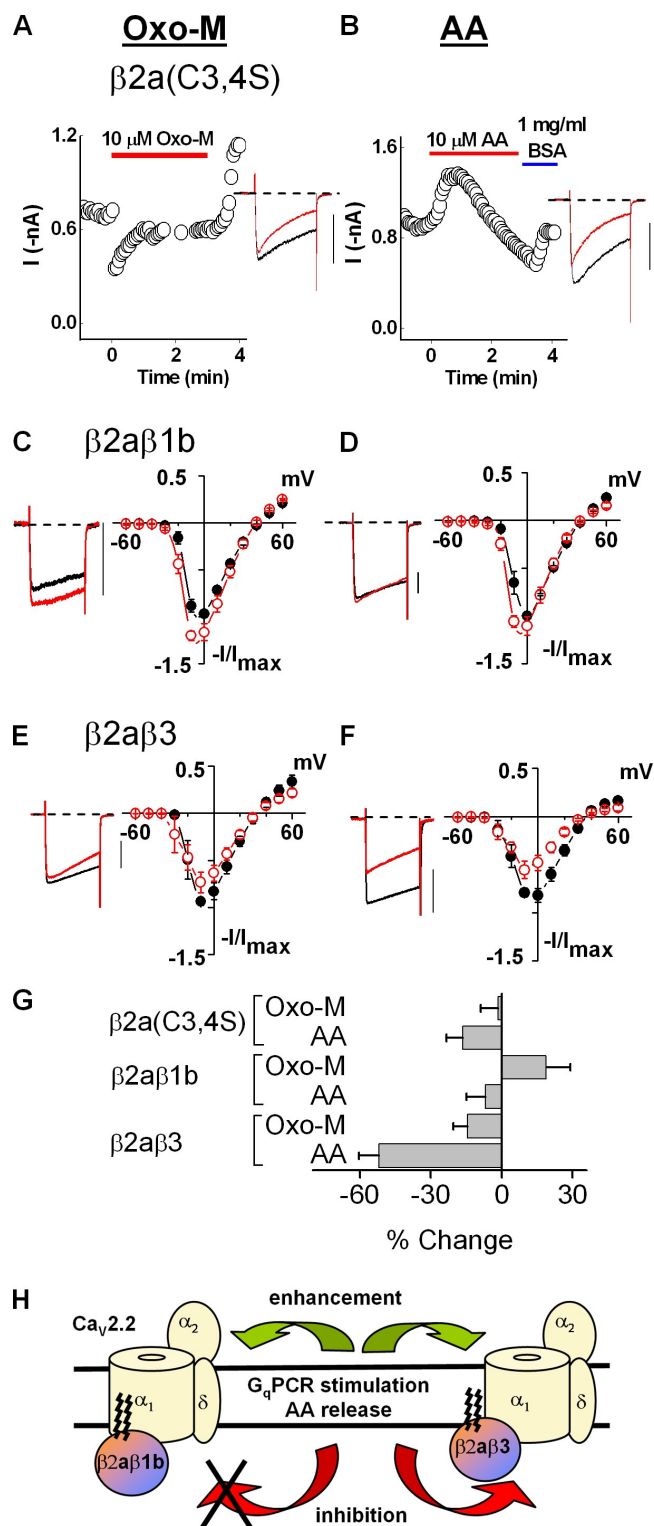
Figure 6. Palmitoylation determines which form of modulation is observed. (A–F) Using 20 mM Ba^{2+}, modulation by Oxo-M or AA of cells expressing mutant Ca$_V$β2a(C3,4S) (A and B), Ca$_V$β2aβ1b (C and D), or Ca$_V$β2aβ3 (E and F) is shown in current traces and I-V plots. Bars, 0.4 nA. (G) Summary of the modulatory effects on currents after application of Oxo-M or AA for 3 min ($n = 4$–7). Error bars represent SEM. (H) Schematic representation of working model.

initial transient inhibition after Oxo-M that relaxed, yielding a small but insignificant inhibition (Fig. 6, A and G). AA initially enhanced current amplitude, followed by significant inhibition (Fig. 6, B and G). The loss of enhancement and appearance of inhibition, although differing in magnitude with Oxo-M or AA, support the idea that palmitoylation blocks inhibition.

If palmitoylation is necessary for antagonizing inhibition, palmitoylating another $Ca_V\beta$ should convert current inhibition to enhancement. Therefore, we tested a chimera in which the variable N terminus of $Ca_V\beta1b$ was replaced with the palmitoylated 16–amino acid N terminus of $Ca_V\beta2a$ ($Ca_V\beta2a\beta1b$; Chien et al., 1998). In cells expressing $Ca_V\beta2a\beta1b$, application of Oxo-M enhanced current with no inhibition (Fig. 6 G). Moreover, AA no longer inhibited these currents significantly (Fig. 6 G) compared with $Ca_V\beta1b$ ($n = 4$; Fig. 2 J). The difference in modulation by AA and Oxo-M may be attributed to an exaggerated response to exogenous application of AA compared with the response to physiological concentrations of AA released upon M_1R stimulation. I-V plots after either Oxo-M or AA exhibited enhancement of current at negative test potentials and no inhibition at positive test potentials (Fig. 6, C and D), suggesting that the palmitoylated N terminus is both necessary and sufficient to block inhibition.

However, a second chimera in which the N terminus of $Ca_V\beta3$ was replaced with the N terminus of $Ca_V\beta2a$ ($Ca_V\beta2a\beta3$; Chien et al., 1998) did not block inhibition as effectively. In cells expressing $Ca_V\beta2a\beta3$, inhibition by Oxo-M was diminished compared with wild-type $Ca_V\beta3$, whereas AA reversibly inhibited currents similarly to wild-type levels (Fig. 6, E–G). I-V plots taken before and 90 s after application of Oxo-M or AA exhibited inhibition at positive test potentials (Fig. 6, E and F). These results indicate that addition of $Ca_V\beta2a$'s palmitoylated N terminus to $Ca_V\beta3$ only partially reproduced the stable enhancement by Oxo-M or AA normally observed with wild-type $Ca_V\beta2a$. Because $Ca_V\beta2a$ protein shares highest sequence homology to $Ca_V\beta1b$ (Birnbaumer et al., 1998), the simplest interpretation for the varied results with the different chimeras is that that $Ca_V\beta2a\beta1b$ positions the palmitoylated N terminus so that it minimizes N-current inhibition similarly to wild-type $Ca_V\beta2a$. In contrast, the more divergent $Ca_V\beta2a\beta3$ positions the palmitoylated N terminus in a different position relative to $Ca_V2.2$ where it is less effective in minimizing inhibition (Fig. 6 H). In support of this notion, $Ca_V\beta2a\beta3$-containing cells exhibited varied kinetics, from noninactivating currents resembling $Ca_V\beta2a$-containing channel activity (Fig. 2 B) to rapidly inactivating currents resembling depalmitoylated $Ca_V\beta2a$-containing channel activity (Fig. 6, A and B). Moreover, the kinetics varied within individual recordings and from cell to cell from a rapidly inactivating to a noninactivating kinetic profile (unpublished data). The unstable inactivation kinetics
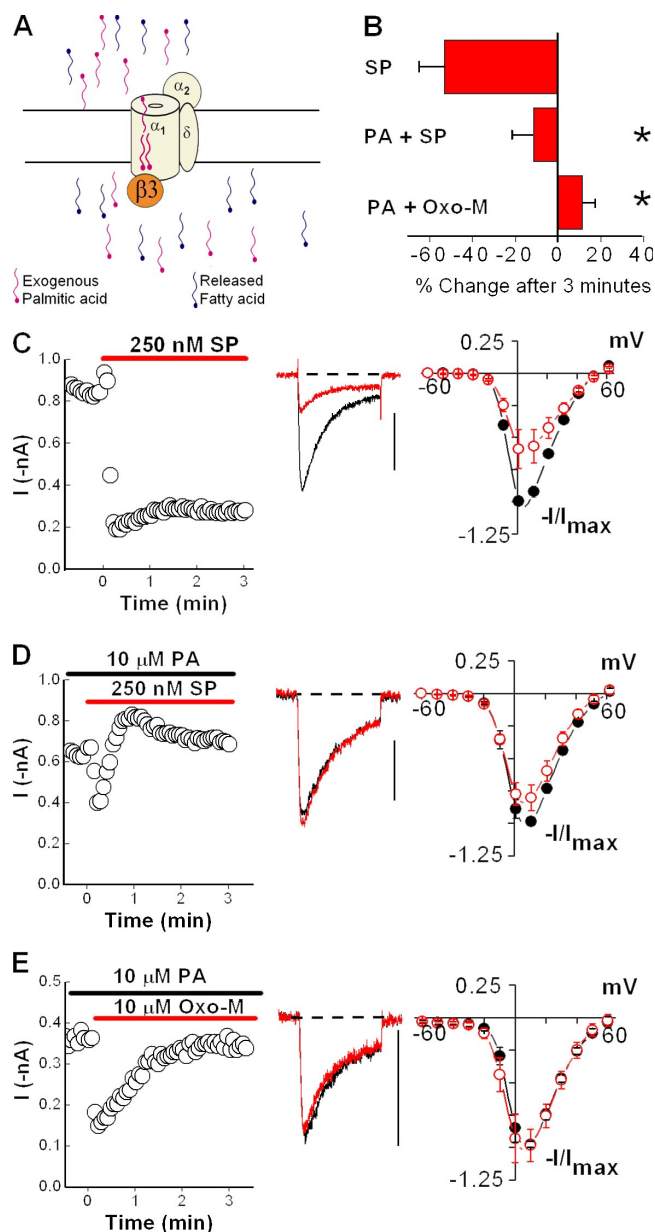

Figure 7. Palmitic acid antagonizes inhibition of N current by G_qPCR stimulation. HEK-M1 cells were transiently transfected with NK-1R, $Ca_V2.2$, $\alpha_2\delta$-1, and $Ca_V\beta3$. (A) Diagram showing that pre-incubation of HEK-M1 cells with exogenously applied palmitic acid blocks inhibition of N channels by fatty acids, such as AA, released after NK-1R or M_1R activation. (B) Summary showing preincubation of cells with 10 µM palmitic acid (PA) significantly attenuates inhibition by SP or Oxo-M (*, P < 0.05 compared with percent change in the absence of palmitic acid). Error bars represent SEM. (C) Modulation of N current by SP from cells expressing $Ca_V\beta3$ is shown in a representative time course, current traces taken before and 3 min after application of SP, and I-V plots ($n = 5$). (D) Pre-incubation of cells with palmitic acid causes loss of inhibition by SP as shown in a time course, current traces, and I-V plot ($n = 6$). (E) Preincubation of HEK-M1 cells with palmitic acid also causes loss of inhibition by Oxo-M, as shown in a representative time course, current traces, and I-V plots ($n = 4$). Bars, 0.4 nA.

suggests that $Ca_V\beta 2a\beta 3$ cannot dock properly to $Ca_V2.2$, thus destabilizing and changing the location of the chimera's palmitoyl groups.

Free palmitic acid minimizes N-current inhibition

If our interpretation that the palmitoyl groups antagonize inhibition is correct, freeing the palmitoyl groups from protein constraints might allow the fatty acids to find and assume their optimal position for blocking inhibition (Fig. 7 A). Alternatively, if the palmitic acids do not interact directly with $Ca_V2.2$, introducing free palmitic acid should not alter N-channel modulation by agonist. We tested this prediction first by preincubating cells expressing NK-1Rs and $Ca_V\beta 3$-containing channels with free palmitic acid for at least 8 min. Under these conditions, the sustained inhibition normally observed with SP (Fig. 7, B and C) was replaced by an initial enhancement that relaxed, resulting in no significant change ($P > 0.24$) in current amplitude over time (Fig. 7, B and D). Moreover, compared with control conditions, little inhibition by SP was detected in I-V plots from cells preincubated with 10 µM palmitic acid (Fig. 7, C and D). To ensure the block of inhibition was not specific to NK-1Rs, we tested N-current modulation of $Ca_V\beta 3$-containing channels in HEK-M1 cells by Oxo-M after a 10-min preincubation with 10 µM palmitic acid. As with SP, free palmitic acid prevented the sustained inhibition observed in its absence, as demonstrated by time courses and I-V plots (compare Fig. 7, B and E with Fig. 1, B–F and Fig. 2, C and E). Bath application of palmitic acid for 8 min did not significantly affect N current (not depicted) when compared with currents recorded under control conditions (Fig. 7 C), indicating that palmitic acid itself has no modulatory effect. These findings demonstrate that exogenous application of free palmitic acid suffices to block current inhibition of $Ca_V\beta 3$-containing N channels. More importantly, these results indicate palmitic acid is both necessary and sufficient to antagonize N-current inhibition during G_qPCR stimulation (Fig. 8).

DISCUSSION

In this study, we used a recombinant system to investigate the enhancement and inhibition of N current that occurs during M_1R stimulation and AA application. In so doing, we made the discovery that the N-channel's β subunit directs opposite effects of N-current modulation. Specifically, M_1R stimulation or exogenous AA uniquely enhanced whole-cell N current from cells expressing $Ca_V\beta 2a$ but inhibited N current from cells expressing $Ca_V\beta 1b$, $Ca_V\beta 3$, or $Ca_V\beta 4$. This finding allowed us to further examine the modulation of N current and reach several additional conclusions. First, the striking recapitulation of M_1R-induced modulation by AA, coupled with the loss of modulation when AA release by
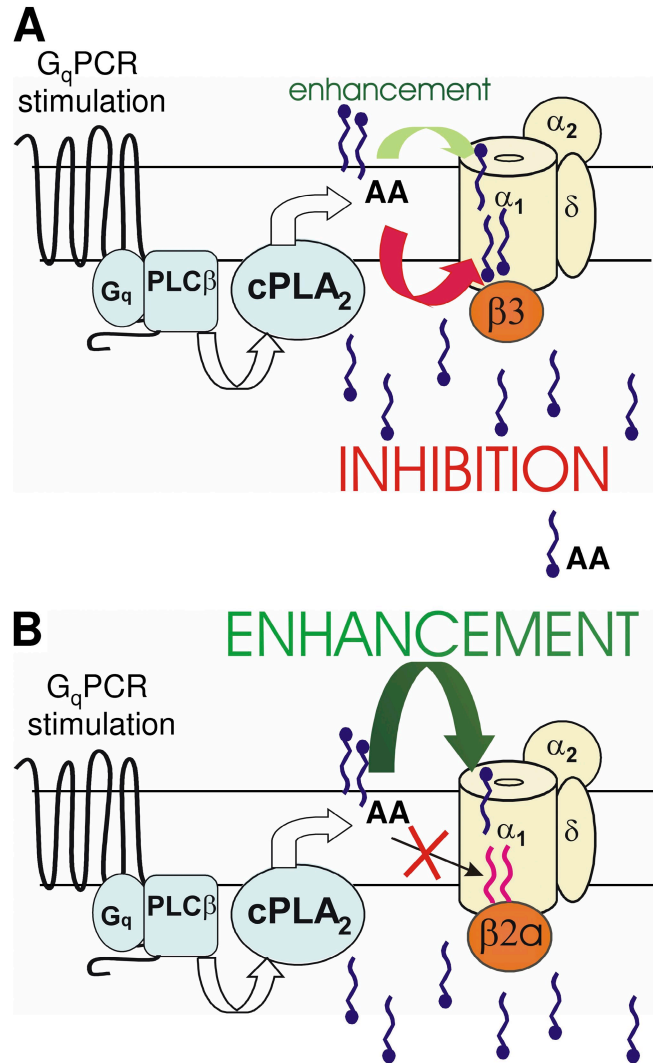

Figure 8. Model of interference of inhibition by palmitoylated $Ca_V\beta 2a$. (A) As presented, our data support a model in which upon G_qPCR stimulation, release of AA initially enhances N current by acting at a site distinct from inhibition. However, N-current inhibition by AA of channels containing $Ca_V\beta 1b$, $Ca_V\beta 3$, or $Ca_V\beta 4$ dominates modulation of $Ca_V2.2$ and obscures enhancement. (B) In the presence of $Ca_V\beta 2a$, the palmitoylated N terminus of the $Ca_V\beta$ subunit blocks N-current inhibition by endogenously released AA as a result of the two palmitic acids competitively interacting with $Ca_V2.2$, thus revealing latent enhancement.

OPC is blocked, is strong evidence that AA is an integral component of the slow pathway. Second, NK-1R stimulation exhibited a similar dual effect, indicating this unique profile of modulation may be conserved among G_qPCRs. Third, cells expressing multiple forms of $Ca_V\beta$ subunits matched the modulatory profile of SCG neurons under the same recording conditions, implying that the characteristic pattern of modulation observed in SCG neurons results from $Ca_V2.2$ coupling with different $Ca_V\beta$ isoforms. This finding provides an explanation of how stimulation of M_1Rs or exogenous AA can elicit both enhancement and inhibition

of N current in individual sympathetic neurons (Liu and Rittenhouse, 2003a). Fourth, using mutated and chimeric $Ca_V\beta$ constructs, we demonstrated that palmitoylation of $Ca_V\beta2a$ is a key feature in its capacity to toggle modulation from inhibition to enhancement. Finally, exogenous application of palmitic acid prevented the characteristic N-current modulation by G_qPCRs, suggesting that $Ca_V\beta2a$'s palmitoyl groups interfere with a mechanism or mechanisms within the slow pathway.

Increased free AA appears necessary for N-current inhibition by the slow pathway

It is well documented that $PtdIns(4,5)P_2$ breakdown by PLC is necessary for slow pathway inhibition (Wu et al., 2002; Liu and Rittenhouse, 2003a; Gamper et al., 2004; Liu et al., 2004; Delmas et al., 2005; Suh and Hille, 2005); however, whether its breakdown is sufficient for N-current inhibition remains controversial (Wu et al., 2002; Gamper et al., 2004; Suh and Hille, 2005). Our data indicate that fatty acid liberation is both necessary and sufficient to elicit inhibition of $Ca_V2.2$ (Barrett et al., 2001; Liu and Rittenhouse, 2003a; Liu et al., 2004, 2007). To demonstrate a role for free AA in N-current inhibition, we used pharmacological agents, the AA scavenger BSA, PLA_2 antibodies dialyzed internally, and neurons harvested from $PLA_2^{-/-}$ knockout mice (Liu and Rittenhouse, 2003a; Liu et al., 2004, 2006). Here we have taken a molecular approach in which expression of palmitoylated $Ca_V\beta2a$ provides a highly specific agent to block inhibition by AA, whereas nonpalmitoylated wild-type $Ca_V\beta$ subunits conveniently act as negative controls. It must be stressed that none of the findings reported here minimizes $PtdIns(4,5)P_2$'s role but rather documents a requirement for AA in N-current inhibition.

A resolution to the paradox would entail a role for both $PtdIns(4,5)P_2$ and AA acting either directly or indirectly on the channel. A model for $PtdIns(4,5)P_2$ and AA opposing each other in modulation of K^+ channels has been published (Oliver et al., 2004) in which $PtdIns(4,5)P_2$ and AA act at different sites of the channel. Direct competition is possible because AA is an integral piece of the $PtdIns(4,5)P_2$ molecule, normally residing in the sn-2 position, and thus could compete for binding to $Ca_V2.2$. Although indirect actions of $PtdIns(4,5)P_2$ and AA must be considered, as both are bioactive molecules with multiple downstream effects, no requirement for downstream enzymes such as phosphatases or kinases has been found. Moreover, antagonizing enzymes that further metabolize AA have no effect on modulation (Liu et al., 2001; Liu and Rittenhouse, 2003a). Nevertheless, increased levels of $PtdIns(4,5)P_2$ increase N-channel availability to open, whereas increased levels of AA stabilize N channels in closed and/or inactivated states (Liu and Rittenhouse, 2000; Gamper et al., 2004). These opposing effects suggest competition.

A working model for enhancement and inhibition

By exposing SCG neurons to exogenous AA, we characterized N-current enhancement and inhibition as distinct molecular events acting at different sites on N channels. Restriction of AA movement across the cell membrane suggested that enhancement requires AA on the extracellular side or within the outer leaflet, whereas inhibition requires AA on the intracellular side or within the inner leaflet (Barrett et al., 2001). These two sites presumably would be equally accessible to AA generated internally because movement of long-chain fatty acids across cell membranes occurs in <1 s (Hamilton et al., 2002). Because $Ca_V\beta$ subunits are cytoplasmic, we hypothesized that $Ca_V\beta2a$ attenuates inhibition without affecting enhancement. In dissociated neurons, AA induces an initial current enhancement followed by a slower progressing inhibition (Barrett et al., 2001; Liu et al., 2001). The simplest explanation for these data is that the initial enhancement becomes masked by the subsequent, more dominant, inhibition. Because previous work indicated that enhancement stems from increased voltage sensitivity (Barrett et al., 2001), we used normalized G-V curves (Fig. 5) to show that an increase in voltage sensitivity occurs independently of $Ca_V\beta2a$ expression. In contrast, inhibition results from an increase in a slow form of inactivation most likely as a result of increased dwell time in one or more intermediate closed states (Liu and Rittenhouse, 2000). This type of inhibition would essentially reduce the available number of channels providing calcium influx, dominating an enhancement produced by a shift in voltage sensitivity. Thus, by blocking a dominant inhibition, $Ca_V\beta2a$ unmasks a latent enhancement. The masking of enhancement offers some explanation for the finding that the majority of studies on N-current modulation have observed inhibition (Elmslie, 2003).

Nevertheless, enhancement and inhibition have been reported from experimental systems similar to the one used here. For example, AA both shifts activation toward negative potentials and simultaneously increases steady-state inactivation of T channels (Talavera et al., 2004). Also, in SCG neurons, the amide of AA, anandamide, elicited enhancement at negative potentials and inhibition at positive potentials in I-V plots (Guo and Ikeda, 2004). Enhancement marked by a leftward shift in voltage sensitivity was reported for R-type channels in the hippocampus (Tai et al., 2006), a region in which $Ca_V\beta2$ is highly expressed (Day et al., 1998). Finally, using HEK-293 cells transiently transfected with recombinant M_1Rs and N channels containing $Ca_V\beta3$, an earlier study showed that carbachol inhibited Ca^{2+} current with no obvious enhancement (Melliti et al., 2001). However, I-V curves showed a discernible leftward shift in voltage sensitivity after carbachol.

A new role for palmitoyl groups of palmitoylated proteins
Our data identify a previously unrecognized role for protein palmitoylation in which it serves as the key feature of $Ca_V\beta2a$'s capacity to toggle $Ca_V2.2$ modulation from inhibition to enhancement after stimulation of G_qPCRs. Here and in other systems, palmitoylation targets or anchors proteins to specific membrane domains (Chien et al., 1996; Resh, 2006). Although dynamic palmitoylation of $Ca_V\beta2a$ has been shown to alter the inactivation kinetics of voltage-gated Ca^{2+} channels in bovine chromaffin cells, the assumed mechanism of action is restriction of movement of channel domains by anchoring the $Ca_V\beta2a$ subunit to the membrane (Hurley et al., 2000). This anchoring in some way is thought to impede current inactivation (Restituito et al., 2001). Thus, palmitoylation increases protein stability and efficiency of action but rarely alters the functional properties of proteins. One exception to this generalization is retinal epithelial protein 65 (RPE65), a chaperone protein for all-trans-retinal esters. In this case, palmitoylation not only targets RPE65 to the plasma membrane but also reverses RPE65's binding specificity for vitamin A to all-trans-retinyl ester, consequently affecting how rapidly photoreceptors respond to light (Xue et al., 2004). Thus, palmitoylation qualitatively alters the substrate specificity of the same protein that is reversibly palmitoylated. Here, our data extend the functions of palmitoylation in a new direction by revealing that after stimulation of G_qPCRs, the palmitoyl groups of one protein, $Ca_V\beta2a$, block inhibition of a second protein, $Ca_V2.2$.

Our finding that palmitoylation antagonizes an inhibition mediated by $PtdIns(4,5)P_2$ breakdown and increased free AA (Liu and Rittenhouse, 2003a; Gamper et al., 2004) raises the possibility that dual palmitoyl groups interact directly with $Ca_V2.2$ to antagonize AA's interaction with $Ca_V2.2$ and subsequent inhibition of N-channel activity. The idea that AA may interact directly with Ca^{2+} channels is supported by the finding that M_1R stimulation or application of exogenous AA also inhibits recombinant Ca_V3 currents in whole-cell (Zhang et al., 2000; Talavera et al., 2004; Hildebrand et al., 2007) and ripped-off patch configurations (Chemin et al., 2007). Because Ca_V3 (T type) channels do not require coexpression of $Ca_V\beta$ or $\alpha_2\delta$ to open, T-channel inhibition must occur at a site on the pore-forming subunit. Moreover, AA inhibits T current with a Hill coefficient of 1.6, indicating cooperative binding of at least two AA molecules to T channels (Talavera et al., 2004). Collectively, these findings are consistent with a direct interaction between AA and T channels. AA likely confers N-current inhibition by acting at a homologous site found on many Ca_V channels because native and recombinant Ca_V1, Ca_V2, and Ca_V3 channels exhibit similar changes in gating after AA (Shimada and Somlyo, 1992; Petit-Jacques and Hartzell, 1996; Liu and Rittenhouse, 2000; Vellani et al., 2000; Talavera et al.,

2004; Chemin et al., 2007; Liu, 2007; Roberts-Crowley and Rittenhouse, 2009).

Palmitoylated $Ca_V\beta2a$ may serve as a phospholipid mimic by competing with $PtdIns(4,5)P_2$ and free AA for interaction with $Ca_V2.2$
Under basal conditions, AA normally resides in the sn-2 position of $PtdIns(4,5)P_2$. Because palmitoylated $Ca_V\beta2a$ appears to antagonize the actions of free AA on $Ca_V2.2$, it may also compete with $PtdIns(4,5)P_2$ for interaction with $Ca_V2.2$, the two palmitic acids of $Ca_V\beta2a$ residing in sites normally occupied by the two fatty acid tails of $PtdIns(4,5)P_2$. Consistent with its ability to block N-current inhibition by free AA, palmitoylated $Ca_V\beta2a$ acts as a phospholipid mimic to maintain normal channel activity (Fig. 8). This model is attractive in that it incorporates previous models, which propose that $PtdIns(4,5)P_2$ associates with channels, increasing their availability to open (Wu et al., 2002; Gamper et al., 2004). The model also supports our previous findings (Liu and Rittenhouse, 2003a) that increased free AA confers current inhibition either by displacing $PtdIns(4,5)P_2$ or by remaining associated with channels after phospholipid breakdown (Roberts-Crowley et al., 2009).

Our findings that free palmitic acid blocks inhibition by SP of $Ca_V\beta3$-containing channels or depalmitoylated $Ca_V\beta2a$-containing channels (see Mitra-Ganguli et al. in this issue) is consistent with the idea that the palmitic acids occupy the same sites recognized by AA. Whether $PtdIns(4,5)P_2$ as well as AA compete for the same site of interaction with $Ca_V2.2$ as the palmitoyl groups of $Ca_V\beta2a$ and where the location of that site is awaits future investigation. However, we have observed that whole-cell recombinant current from $Ca_V\beta2a$-containing channels, in contrast to $Ca_V\beta3$-containing channels (Gamper et al., 2004), run down only minimally over time (unpublished data), consistent with palmitoylated $Ca_V\beta2a$ functionally substituting for $PtdIns(4,5)P_2$. Thus, when taken together, our findings and the results of other laboratories best fit a model in which palmitoylated $Ca_V\beta2a$, $PtdIns(4,5)P_2$, and free AA compete for an overlapping interaction site on $Ca_V2.2$. Given the extent that lipids such as $PtdIns(4,5)P_2$ and AA associate with membrane protein complexes (Piomelli, 1993; Doughman et al., 2003), the interference of such interactions by palmitoylated proteins is predicted to occur in other protein complexes, yielding broad importance beyond ion channel functioning.

Expression of palmitoylated $Ca_V\beta2a$ may underlie novel forms of synaptic plasticity
In particular, the presence or absence of palmitoylated $Ca_V\beta2a$ may have far-reaching consequences for synaptic plasticity. $Ca_V\beta2$ expression displays an overlapping distribution with G_qPCRs (Tencé et al., 1994; Liu and Rittenhouse, 2003a) throughout the brain and is

primarily localized postsynaptically in dendrites and cell bodies (Lie et al., 1999), indicating that enhancement of Ca^{2+} channel activity may specifically affect postsynaptic membrane excitability. In support of this notion, increased current amplitude and/or kinetic changes associated with Ca^{2+} current enhancement (Zhang et al., 2000; Bannister et al., 2004; Guo and Ikeda, 2004; Talavera et al., 2004; Tai et al., 2006; Chemin et al., 2007; Mitra-Ganguli et al., 2009) occur in different neurons and recombinant channels from the Ca_V2 and Ca_V3 families (Keyser and Alger, 1990; Melliti et al., 2001; Chemin et al., 2007; Meza et al., 2007). In contrast, native or recombinant channels associated with $Ca_V\beta1b$, $Ca_V\beta3$, or $Ca_V\beta4$ exhibit inhibition after similar stimulation (Keyser and Alger, 1990; Liu and Rittenhouse, 2003a; Gamper et al., 2004; Guo and Ikeda, 2004; Meza et al., 2007). Because $Ca_V\beta2$ expression changes developmentally (Tanaka et al., 1995) and with activity (Lie et al., 1999), postsynaptic responses also may change over time. Patients with temporal lobe epilepsy exhibit increased postsynaptic $Ca_V\beta2$ expression in damaged hippocampal regions. In contrast, patients that underwent surgical lesioning exhibit hippocampal $Ca_V\beta$ levels indistinguishable from control patients (Lie et al., 1999), suggesting $Ca_V\beta2$ expression is dynamically regulated by electrical activity. Moreover, it has been reported that although $Ca_V\beta$ expression appears necessary for surface expression of the N channel, once the channel reaches the cell surface, the $Ca_V\beta$ subunit can be exchanged (Restituito et al., 2001; Hidalgo et al., 2006). Thus, changes in current modulation caused by changes in $Ca_V\beta$ expression should not require a turnover of the entire channel complex.

Whether up-regulation of $Ca_V\beta2$ is a response to counteract hyperexcitability or whether increased $Ca_V\beta2$ levels contribute to excitotoxic neurodegeneration has not been determined. Nevertheless, these findings document in vivo plasticity of $Ca_V\beta2$ expression. In the short term, palmitoyl acyl transferases dynamically regulate protein palmitoylation in hippocampal dendrites and cell bodies to control synaptic function (El-Husseini et al., 2002; Fukata et al., 2004). Pulse–chase experiments using tritiated palmitate indicate that palmitate turns over multiple times during the lifetime of most palmitoylated proteins, and recent experiments suggest that the pulse–chase experiments may underestimate the turnover rate by 15–20-fold as a result of reacylation of proteins by the radiolabeled palmitate within a cell (for review see Baekkeskov and Kanaani, 2009). Thus, expression of $Ca_V\beta2a$ in postsynaptic regions should create a previously unrealized level of plasticity in which the response to a transmitter, acting on its G_qPCR from moment to moment, may switch from inhibitory to excitatory depending on whether $Ca_V\beta2a$'s palmitoyl groups interact with $Ca_V2.2$.

A role for multiple $Ca_V\beta$ isoforms in neurons

In summary, we have shown that multiple $Ca_V\beta$ isoforms expressed in a recombinant system can recapitulate native N-current modulation by the slow pathway. Given the diversity of neuronal functions for calcium influx, there must be localized control of a channel's response to modulation. Our findings provide a previously unrecognized role for $Ca_V\beta$ subunits in the control of modulation and indicate a means by which G_qPCR stimulation can simultaneously up- and down-regulate calcium flux at distinct sites within a single cell. Moreover, our experiments and analyses identify the sites that confer sensitivity to inhibition by AA as a likely site of plasticity.

REFERENCES

Baekkeskov, S., and J. Kanaani. 2009. Palmitoylation cycles and regulation of protein function (Review). *Mol. Membr. Biol.* 26:42–54. doi:10.1080/09687680802680108

Bannister, R.A., K. Melliti, and B.A. Adams. 2004. Differential modulation of CaV2.3 Ca2+ channels by Galphaq/11-coupled muscarinic receptors. *Mol. Pharmacol.* 65:381–388. doi:10.1124/mol.65.2.381

Barrett, C.F., and A.R. Rittenhouse. 2000. Modulation of N-type calcium channel activity by G-proteins and protein kinase C. *J. Gen. Physiol.* 115:277–286. doi:10.1085/jgp.115.3.277

Barrett, C.F., L. Liu, and A.R. Rittenhouse. 2001. Arachidonic acid reversibly enhances N-type calcium current at an extracellular site. *Am. J. Physiol. Cell Physiol.* 280:C1306–C1318.

Beech, D.J., L. Bernheim, and B. Hille. 1992. Pertussis toxin and voltage dependence distinguish multiple pathways modulating calcium channels of rat sympathetic neurons. *Neuron.* 8:97–106. doi:10.1016/0896-6273(92)90111-P

Bernheim, L., A. Mathie, and B. Hille. 1992. Characterization of muscarinic receptor subtypes inhibiting Ca2+ current and M current in rat sympathetic neurons. *Proc. Natl. Acad. Sci. USA.* 89:9544–9548. doi:10.1073/pnas.89.20.9544

Birnbaumer, L., N. Qin, R. Olcese, E. Tareilus, D. Platano, J. Costantin, and E. Stefani. 1998. Structures and functions of calcium channel beta subunits. *J. Bioenerg. Biomembr.* 30:357–375. doi:10.1023/A:1021989622656

Brosenitsch, T.A., and D.M. Katz. 2001. Physiological patterns of electrical stimulation can induce neuronal gene expression by activating N-type calcium channels. *J. Neurosci.* 21:2571–2579.

Catterall, W.A. 2000. Structure and regulation of voltage-gated Ca2+ channels. *Annu. Rev. Cell Dev. Biol.* 16:521–555. doi:10.1146/annurev.cellbio.16.1.521

Chemin, J., J. Nargeot, and P. Lory. 2007. Chemical determinants involved in anandamide-induced inhibition of T-type calcium channels. *J. Biol. Chem.* 282:2314–2323. doi:10.1074/jbc.M610033200

Chien, A.J., and M.M. Hosey. 1998. Post-translational modifications of beta subunits of voltage-dependent calcium channels. *J. Bioenerg. Biomembr.* 30:377–386. doi:10.1023/A:1021941706726

Chien, A.J., K.M. Carr, R.E. Shirokov, E. Rios, and M.M. Hosey. 1996. Identification of palmitoylation sites within the L-type calcium channel beta2a subunit and effects on channel function. *J. Biol. Chem.* 271:26465–26468. doi:10.1074/jbc.271.43.26465

Chien, A.J., T. Gao, E. Perez-Reyes, and M.M. Hosey. 1998. Membrane targeting of L-type calcium channels. Role of palmitoylation in the subcellular localization of the beta2a subunit. *J. Biol. Chem.* 273:23590–23597. doi:10.1074/jbc.273.36.23590

Day, N.C., S.G. Volsen, A.L. McCormack, P.J. Craig, W. Smith, R.E. Beattie, P.J. Shaw, S.B. Ellis, M.M. Harpold, and P.G. Ince. 1998. The expression of voltage-dependent calcium channel beta subunits in human hippocampus. *Brain Res. Mol. Brain Res.* 60:259–269. doi:10.1016/S0169-328X(98)00186-7

Delmas, P., B. Coste, N. Gamper, and M.S. Shapiro. 2005. Phosphoinositide lipid second messengers: new paradigms for calcium channel modulation. *Neuron.* 47:179–182. doi:10.1016/j.neuron.2005.07.001

Doughman, R.L., A.J. Firestone, and R.A. Anderson. 2003. Phosphatidylinositol phosphate kinases put PI4,5P(2) in its place. *J. Membr. Biol.* 194:77–89. doi:10.1007/s00232-003-2027-7

El-Husseini, A.E.-D., E. Schnell, S. Dakoji, N. Sweeney, Q. Zhou, O. Prange, C. Gauthier-Campbell, A. Aguilera-Moreno, R.A. Nicoll, and D.S. Bredt. 2002. Synaptic strength regulated by palmitate cycling on PSD-95. *Cell.* 108:849–863. doi:10.1016/S0092-8674(02)00683-9

Elmslie, K.S. 2003. Neurotransmitter modulation of neuronal calcium channels. *J. Bioenerg. Biomembr.* 35:477–489. doi:10.1023/B:JOBB.0000008021.55853.18

Ford, C.P., P.L. Stemkowski, P.E. Light, and P.A. Smith. 2003. Experiments to test the role of phosphatidylinositol 4,5-bisphosphate in neurotransmitter-induced M-channel closure in bullfrog sympathetic neurons. *J. Neurosci.* 23:4931–4941.

Fukata, M., Y. Fukata, H. Adesnik, R.A. Nicoll, and D.S. Bredt. 2004. Identification of PSD-95 palmitoylating enzymes. *Neuron.* 44:987–996. doi:10.1016/j.neuron.2004.12.005

Gamper, N., V. Reznikov, Y. Yamada, J. Yang, and M.S. Shapiro. 2004. Phosphatidylinositol [correction] 4,5-bisphosphate signals underlie receptor-specific Gq/11-mediated modulation of N-type Ca2+ channels. *J. Neurosci.* 24:10980–10992. doi:10.1523/JNEUROSCI.3869-04.2004

Guo, J.S., and S.R. Ikeda. 2004. Endocannabinoids modulate N-type calcium channels and G-protein-coupled inwardly rectifying potassium channels via CB1 cannabinoid receptors heterologously expressed in mammalian neurons. *Mol. Pharmacol.* 65:665–674. doi:10.1124/mol.65.3.665

Hamilton, J.A., W. Guo, and F. Kamp. 2002. Mechanism of cellular uptake of long-chain fatty acids: do we need cellular proteins? *Mol. Cell. Biochem.* 239:17–23. doi:10.1023/A:1020542220599

Hidalgo, P., G. Gonzalez-Gutierrez, J. Garcia-Olivares, and A. Neely. 2006. The alpha1-beta-subunit interaction that modulates calcium channel activity is reversible and requires a competent alpha-interaction domain. *J. Biol. Chem.* 281:24104–24110. doi:10.1074/jbc.M605930200

Hildebrand, M.E., L.S. David, J. Hamid, K. Mulatz, E. Garcia, G.W. Zamponi, and T.P. Snutch. 2007. Selective inhibition of Cav3.3 T-type calcium channels by Galphaq/11-coupled muscarinic acetylcholine receptors. *J. Biol. Chem.* 282:21043–21055. doi:10.1074/jbc.M611809200

Hurley, J.H., A.L. Cahill, K.P. Currie, and A.P. Fox. 2000. The role of dynamic palmitoylation in Ca2+ channel inactivation. *Proc. Natl. Acad. Sci. USA.* 97:9293–9298. doi:10.1073/pnas.160589697

Kammermeier, P.J., V. Ruiz-Velasco, and S.R. Ikeda. 2000. A voltage-independent calcium current inhibitory pathway activated by muscarinic agonists in rat sympathetic neurons requires both Galpha q/11 and Gbeta gamma. *J. Neurosci.* 20:5623–5629.

Keyser, D.O., and B.E. Alger. 1990. Arachidonic acid modulates hippocampal calcium current via protein kinase C and oxygen radicals. *Neuron.* 5:545–553. doi:10.1016/0896-6273(90)90092-T

Lie, A.A., I. Blümcke, S.G. Volsen, O.D. Wiestler, C.E. Elger, and H. Beck. 1999. Distribution of voltage-dependent calcium channel beta subunits in the hippocampus of patients with temporal lobe epilepsy. *Neuroscience.* 93:449–456. doi:10.1016/S0306-4522(99)00162-1

Lin, Z., C. Harris, and D. Lipscombe. 1996. The molecular identity of Ca channel alpha 1-subunits expressed in rat sympathetic neurons. *J. Mol. Neurosci.* 7:257–267. doi:10.1007/BF02737063

Lin, Z., S. Haus, J. Edgerton, and D. Lipscombe. 1997. Identification of functionally distinct isoforms of the N-type Ca2+ channel in rat sympathetic ganglia and brain. *Neuron.* 18:153–166. doi:10.1016/S0896-6273(01)80054-4

Lin, Y.S., S.I. McDonough, and D. Lipscombe. 2004. Alternative splicing in the voltage-sensing region of N-type CaV2.2 channels modulates channel kinetics. *J. Neurophysiol.* 92:2820–2830. doi:10.1152/jn.00048.2004

Liu, L., and A.R. Rittenhouse. 2000. Effects of arachidonic acid on unitary calcium currents in rat sympathetic neurons. *J. Physiol.* 525:391–404. doi:10.1111/j.1469-7793.2000.00391.x

Liu, L., and A.R. Rittenhouse. 2003a. Arachidonic acid mediates muscarinic inhibition and enhancement of N-type Ca2+ current in sympathetic neurons. *Proc. Natl. Acad. Sci. USA.* 100:295–300. doi:10.1073/pnas.0136826100

Liu, L., and A.R. Rittenhouse. 2003b. Pharmacological discrimination between muscarinic receptor signal transduction cascades with bethanechol chloride. *Br. J. Pharmacol.* 138:1259–1270. doi:10.1038/sj.bjp.0705157

Liu, L.C., C.F. Barrett, and A.R. Rittenhouse. 2001. Arachidonic acid both inhibits and enhances whole cell calcium currents in rat sympathetic neurons. *Am. J. Physiol. Cell Physiol.* 280:C1293–C1305.

Liu, L.P., P.K. Gonzalez, C.F. Barrett, and A.R. Rittenhouse. 2003. The calcium channel ligand FPL 64176 enhances L-type but inhibits N-type neuronal calcium currents. *Neuropharmacology.* 45:281–292. doi:10.1016/S0028-3908(03)00153-9

Liu, L., M.L. Roberts, and A.R. Rittenhouse. 2004. Phospholipid metabolism is required for M1 muscarinic inhibition of N-type calcium current in sympathetic neurons. *Eur. Biophys. J.* 33:255–264. doi:10.1007/s00249-003-0387-7

Liu, L., R. Zhao, Y. Bai, L.F. Stanish, J.E. Evans, M.J. Sanderson, J.V. Bonventre, and A.R. Rittenhouse. 2006. M1 muscarinic receptors inhibit L-type Ca2+ current and M-current by divergent signal transduction cascades. *J. Neurosci.* 26:11588–11598. doi:10.1523/JNEUROSCI.2102-06.2006

Liu, L.J., J.F. Heneghan, T. Mitra-Ganguli, M.L. Roberts-Crowley, and A.R. Rittenhouse. 2007. Role of PIP2 in regulating versus modulating Ca2+ channel activity. *J. Physiol.* 583:1165–1166; author reply 1167. doi:10.1113/jphysiol.2007.141424

Liu, L.J., J.F. Heneghan, G.J. Michael, L.F. Stanish, M. Egertová, and A.R. Rittenhouse. 2008. L- and N-current but not M-current inhibition by M1 muscarinic receptors requires DAG lipase activity. *J. Cell. Physiol.* 216:91–100. doi:10.1002/jcp.21378

Liu, S.J. 2007. Inhibition of L-type Ca2+ channel current and negative inotropy induced by arachidonic acid in adult rat

ventricular myocytes. *Am. J. Physiol. Cell Physiol.* 293:C1594–C1604. doi:10.1152/ajpcell.00284.2007

Macdonald, S.G., J.J. Dumas, and N.D. Boyd. 1996. Chemical cross-linking of the substance P (NK-1) receptor to the alpha subunits of the G proteins Gq and G11. *Biochemistry.* 35:2909–2916. doi:10.1021/bi952351+

Mathie, A., L. Bernheim, and B. Hille. 1992. Inhibition of N- and L-type calcium channels by muscarinic receptor activation in rat sympathetic neurons. *Neuron.* 8:907–914. doi:10.1016/0896-6273(92)90205-R

Melliti, K., U. Meza, and B.A. Adams. 2001. RGS2 blocks slow muscarinic inhibition of N-type Ca(2+) channels reconstituted in a human cell line. *J. Physiol.* 532:337–347. doi:10.1111/j.1469-7793.2001.0337f.x

Meza, U., A. Thapliyal, R.A. Bannister, and B.A. Adams. 2007. Neurokinin 1 receptors trigger overlapping stimulation and inhibition of CaV2.3 (R-type) calcium channels. *Mol. Pharmacol.* 71:284–293. doi:10.1124/mol.106.028530

Michailidis, I.E., Y. Zhang, and J. Yang. 2007. The lipid connection-regulation of voltage-gated Ca(2+) channels by phosphoinositides. *Pflugers Arch.* 455:147–155. doi:10.1007/s00424-007-0272-9

Mitra-Ganguli, T., I. Vitko, E. Perez-Reyes, and A.R. Rittenhouse. 2009. Orientation of palmitoylated CaVβ2a relative to CaV2.2 is critical for slow pathway modulation of N-type Ca^{2+} current by tachykinin receptor activation. *J. Gen. Physiol.* 134:385–396.

Olcese, R., N. Qin, T. Schneider, A. Neely, X. Wei, E. Stefani, and L. Birnbaumer. 1994. The amino terminus of a calcium channel beta subunit sets rates of channel inactivation independently of the subunit's effect on activation. *Neuron.* 13:1433–1438. doi:10.1016/0896-6273(94)90428-6

Oliver, D.C., C.C. Lien, M. Soom, T. Baukrowitz, P. Jonas, and B. Fakler. 2004. Functional conversion between A-type and delayed rectifier K+ channels by membrane lipids. *Science.* 304:265–270. doi:10.1126/science.1094113

Peralta, E.G., A. Ashkenazi, J.W. Winslow, J. Ramachandran, and D.J. Capon. 1988. Differential regulation of PI hydrolysis and adenylyl cyclase by muscarinic receptor subtypes. *Nature.* 334:434–437. doi:10.1038/334434a0

Perez, J.F., and M.J. Sanderson. 2005. The frequency of calcium oscillations induced by 5-HT, ACH, and KCl determine the contraction of smooth muscle cells of intrapulmonary bronchioles. *J. Gen. Physiol.* 125:535–553. doi:10.1085/jgp.200409216

Petit-Jacques, J.H., and H.C. Hartzell. 1996. Effect of arachidonic acid on the L-type calcium current in frog cardiac myocytes. *J. Physiol.* 493:67–81.

Piomelli, D. 1993. Arachidonic acid in cell signaling. *Curr. Opin. Cell Biol.* 5:274–280. doi:10.1016/0955-0674(93)90116-8

Plummer, M.R., D.E. Logothetis, and P. Hess. 1989. Elementary properties and pharmacological sensitivities of calcium channels in mammalian peripheral neurons. *Neuron.* 2:1453–1463. doi:10.1016/0896-6273(89)90191-8

Pragnell, M., M. De Waard, Y. Mori, T. Tanabe, T.P. Snutch, and K.P. Campbell. 1994. Calcium channel beta-subunit binds to a conserved motif in the I-II cytoplasmic linker of the alpha 1-subunit. *Nature.* 368:67–70. doi:10.1038/368067a0

Resh, M.D. 2006. Palmitoylation of ligands, receptors, and intracellular signaling molecules. *Sci. STKE.* doi:10.1126/stke.3592006re14

Restituito, S., T. Cens, M. Rousset, and P. Charnet. 2001. Ca(2+) channel inactivation heterogeneity reveals physiological unbinding of auxiliary beta subunits. *Biophys. J.* 81:89–96. doi:10.1016/S0006-3495(01)75682-2

Rittenhouse, A.R., and R.E. Zigmond. 1999. Role of N- and L-type calcium channels in depolarization-induced activation of tyrosine hydroxylase and release of norepinephrine by sympathetic cell bodies and nerve terminals. *J. Neurobiol.* 40:137–148. doi:10.1002/(SICI)1097-4695(199908)40:2<137::AID-NEU1>3.0.CO;2-A

Roberts-Crowley, M.L., and A.R. Rittenhouse. 2009. Arachidonic acid inhibition of L-type calcium (CaV1.3b) channels varies with accessory CaVβ subunits. *J. Gen. Physiol.* 133:387–403. doi:10.1085/jgp.200810047

Roberts-Crowley, M.L., T. Mitra-Ganguli, L. Liu, and A.R. Rittenhouse. 2009. Regulation of voltage-gated Ca2+ channels by lipids. *Cell Calcium.* 45:589–601. doi:10.1016/j.ceca.2009.03.015

Sanderson, M.J., and I. Parker. 2003. Video-rate confocal microscopy. *Methods Enzymol.* 360:447–481. doi:10.1016/S0076-6879(03)60123-0

Scott, V.E., M. De Waard, H. Liu, C.A. Gurnett, D.P. Venzke, V.A. Lennon, and K.P. Campbell. 1996. Beta subunit heterogeneity in N-type Ca2+ channels. *J. Biol. Chem.* 271:3207–3212. doi:10.1074/jbc.271.6.3207

Shapiro, M.S., and B. Hille. 1993. Substance P and somatostatin inhibit calcium channels in rat sympathetic neurons via different G protein pathways. *Neuron.* 10:11–20. doi:10.1016/0896-6273(93)90237-L

Shapiro, M.S., L.P. Wollmuth, and B. Hille. 1994. Modulation of Ca2+ channels by PTX-sensitive G-proteins is blocked by N-ethylmaleimide in rat sympathetic neurons. *J. Neurosci.* 14:7109–7116.

Shimada, T.A., and A.P. Somlyo. 1992. Modulation of voltage-dependent Ca channel current by arachidonic acid and other long-chain fatty acids in rabbit intestinal smooth muscle. *J. Gen. Physiol.* 100:27–44. doi:10.1085/jgp.100.1.27

Spector, A.A. 1975. Fatty acid binding to plasma albumin. *J. Lipid Res.* 16:165–179.

Suh, B.C., and B. Hille. 2002. Recovery from muscarinic modulation of M current channels requires phosphatidylinositol 4,5-bisphosphate synthesis. *Neuron.* 35:507–520. doi:10.1016/S0896-6273(02)00790-0

Suh, B.C., and B. Hille. 2005. Regulation of ion channels by phosphatidylinositol 4,5-bisphosphate. *Curr. Opin. Neurobiol.* 15:370–378. doi:10.1016/j.conb.2005.05.005

Suh, B.C., and B. Hille. 2007. Regulation of KCNQ channels by manipulation of phosphoinositides. *J. Physiol.* 582:911–916. doi:10.1113/jphysiol.2007.132647

Suh, B.C., T. Inoue, T. Meyer, and B. Hille. 2006. Rapid chemically induced changes of PtdIns(4,5)P2 gate KCNQ ion channels. *Science.* 314:1454–1457. doi:10.1126/science.1131163

Tai, C., J.B. Kuzmiski, and B.A. MacVicar. 2006. Muscarinic enhancement of R-type calcium currents in hippocampal CA1 pyramidal neurons. *J. Neurosci.* 26:6249–6258. doi:10.1523/JNEUROSCI.1009-06.2006

Talavera, K., M. Staes, A. Janssens, G. Droogmans, and B. Nilius. 2004. Mechanism of arachidonic acid modulation of the T-type Ca2+ channel α1G. *J. Gen. Physiol.* 124:225–238. doi:10.1085/jgp.200409050

Tanaka, O., H. Sakagami, and H. Kondo. 1995. Localization of mRNAs of voltage-dependent Ca(2+)-channels: four subtypes of alpha 1- and beta-subunits in developing and mature rat brain. *Brain Res. Mol. Brain Res.* 30:1–16. doi:10.1016/0169-328X(94)00265-G

Tencé, M., J. Cordier, J. Premont, and J. Glowinski. 1994. Muscarinic cholinergic agonists stimulate arachidonic acid release from mouse striatal neurons in primary culture. *J. Pharmacol. Exp. Ther.* 269:646–653.

Vellani, V.A., A.M. Reynolds, and P.A. McNaughton. 2000. Modulation of the synaptic Ca2+ current in salamander photoreceptors by polyunsaturated fatty acids and retinoids. *J. Physiol.* 529:333–344. doi:10.1111/j.1469-7793.2000.00333.x

West, A.E., W.G. Chen, M.B. Dalva, R.E. Dolmetsch, J.M. Kornhauser, A.J. Shaywitz, M.A. Takasu, X. Tao, and M.E. Greenberg. 2001. Calcium regulation of neuronal gene expression. *Proc. Natl. Acad. Sci. USA.* 98:11024–11031. doi:10.1073/pnas.191352298

Wisgirda, M.E., and S.E. Dryer. 1994. Functional dependence of Ca(2+)-activated K+ current on L- and N-type Ca2+ channels:

differences between chicken sympathetic and parasympathetic neurons suggest different regulatory mechanisms. *Proc. Natl. Acad. Sci. USA.* 91:2858–2862. doi:10.1073/pnas.91.7.2858

Witcher, D.R., M. De Waard, J. Sakamoto, C. Franzini-Armstrong, M. Pragnell, S.D. Kahl, and K.P. Campbell. 1993. Subunit identification and reconstitution of the N-type Ca2+ channel complex purified from brain. *Science.* 261:486–489. doi:10.1126/science.8392754

Wu, L.C., C.S. Bauer, X.G. Zhen, C. Xie, and J. Yang. 2002. Dual regulation of voltage-gated calcium channels by PtdIns(4,5)P2. *Nature.* 419:947–952. doi:10.1038/nature01118

Xue, L.D., D.R. Gollapalli, P. Maiti, W.J. Jahng, and R.R. Rando. 2004. A palmitoylation switch mechanism in the regulation of the visual cycle. *Cell.* 117:761–771. doi:10.1016/j.cell.2004.05.016

Yasuda, T., L. Chen, W. Barr, J.E. McRory, R.J. Lewis, D.J. Adams, and G.W. Zamponi. 2004. Auxiliary subunit regulation of high-voltage activated calcium channels expressed in mammalian cells. *Eur. J. Neurosci.* 20:1–13. doi:10.1111/j.1460-9568.2004.03434.x

Zhang, Y.L., L.L. Cribbs, and J. Satin. 2000. Arachidonic acid modulation of alpha1H, a cloned human T-type calcium channel. *Am. J. Physiol. Heart Circ. Physiol.* 278:H184–H193.

Zhao, R., L. Liu, and A.R. Rittenhouse. 2007. Ca2+ influx through both L- and N-type Ca2+ channels increases c-fos expression by electrical stimulation of sympathetic neurons. *Eur. J. Neurosci.* 25:1127–1135. doi:10.1111/j.1460-9568.2007.05359.x